Chirality in odd-odd nuclei: simple models and experimental results

NORDITA: Chiral Bands in Nuclei

Krzysztof Starosta

Simon Fraser University
starosta@sfu.ca

April 20, 2015

Outline

1. Early in the game

Outline

1. Early in the game
2. Why was/is chirality exciting?

Outline

1. Early in the game
2. Why was/is chirality exciting?
3. What have we learned?

Outline

1. Early in the game
2. Why was/is chirality exciting?
3. What have we learned?
4. Circumstantial evidence

Outline

1. Early in the game
2. Why was/is chirality exciting?
3. What have we learned?
4. Circumstantial evidence
5. Can we nail it down?

Outline

1. Early in the game
2. Why was/is chirality exciting?
3. What have we learned?
4. Circumstantial evidence
5. Can we nail it down?
6. Opportunities at TRIUMF

Outline

Outline

1. Early in the game
2. Why was/is chirality exciting?
3. What have we learned?
4. Circumstantial evidence
5. Can we nail it down?
6. Opportunities at TRIUMF
7. Possible experiments
8. Can we find the smoking gun?

Early in the game

NSCL SUNY Stony Brook ∼2000

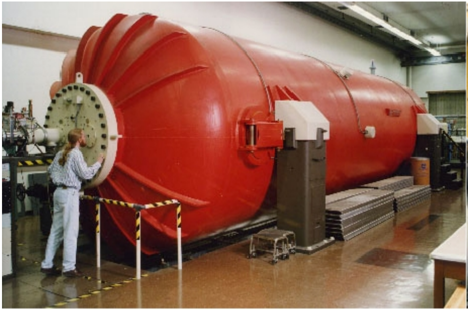

Early in the game

Early in the game

David Fossan
1934-2003

Experimental searches

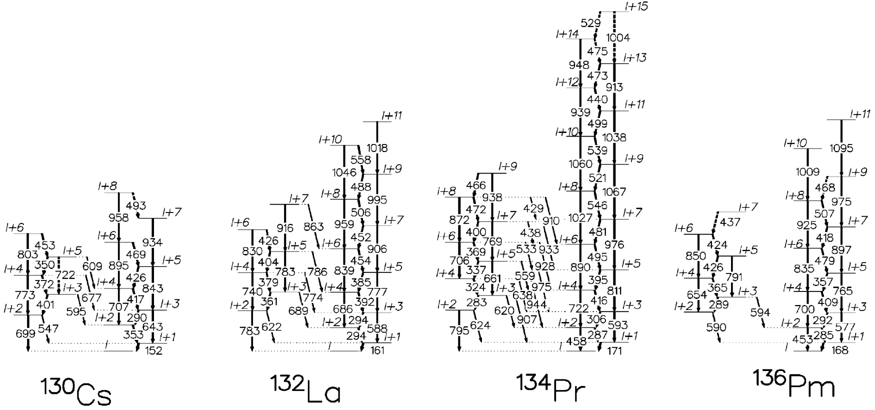

Geometry calculations

- *the Hamiltonian:*

$$H = \sum_{\tau\alpha} \varepsilon_{\tau\alpha} a^{+}_{\tau\alpha} a_{\tau\alpha} - \frac{1}{2} \sum_{\tau\tau'} \chi_{\tau\tau'} \sum_{m} Q^{+}_{m}(\tau) Q_{m}(\tau'),$$

$$Q_m(\tau) = \frac{1}{\sqrt{5}} \sum_{\sigma_\alpha \sigma_\beta} q(\tau\alpha, \tau\beta) [a^{+}_{\tau\alpha} \widetilde{a}_{\tau\beta}]_{2m},$$

- *the basis:*

$$\left| \Phi_{IK}(\lambda, \mu, L, R, r, t) \right\rangle = \left[[a^{+}_{\tau\alpha} \widetilde{a}_{\tau\beta}]_{LM} \left| R, r, t \right\rangle \right]_{IK},$$

- *the Kerman–Klein Dönau–Frauendorf method*

$$H = H^{coll.}_{core} + H^{sp}_{\pi} + H^{sp.}_{\nu} + H^{QQ}_{core-\pi} + H^{QQ}_{core-\nu} + H^{QQ}_{\pi-\nu}.$$

Geometry calculations

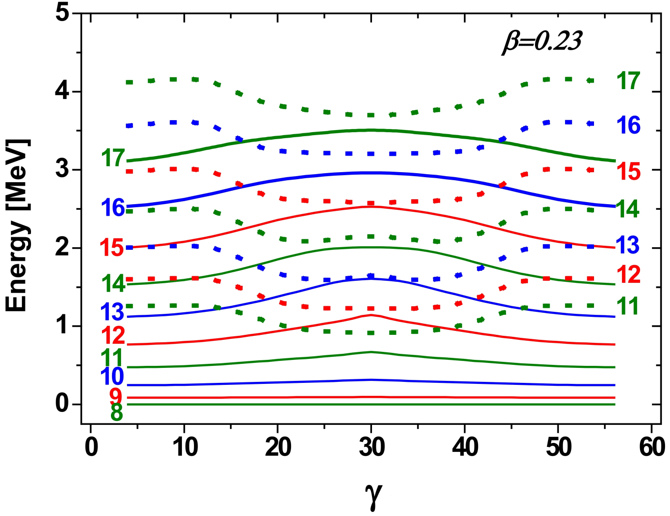

Geometry calculations

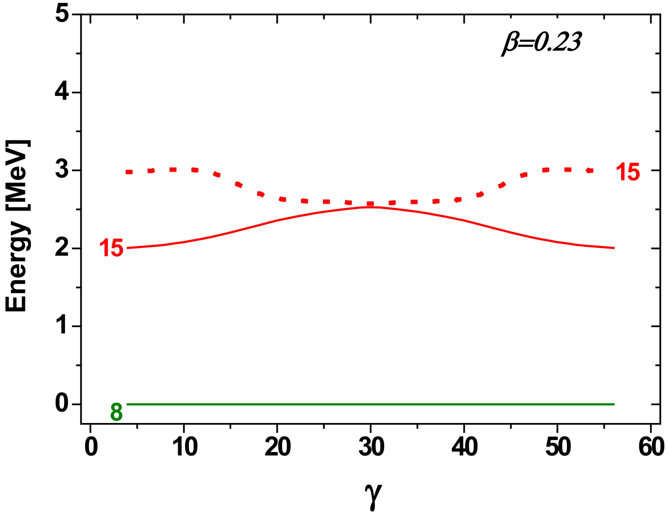

Geometry calculations

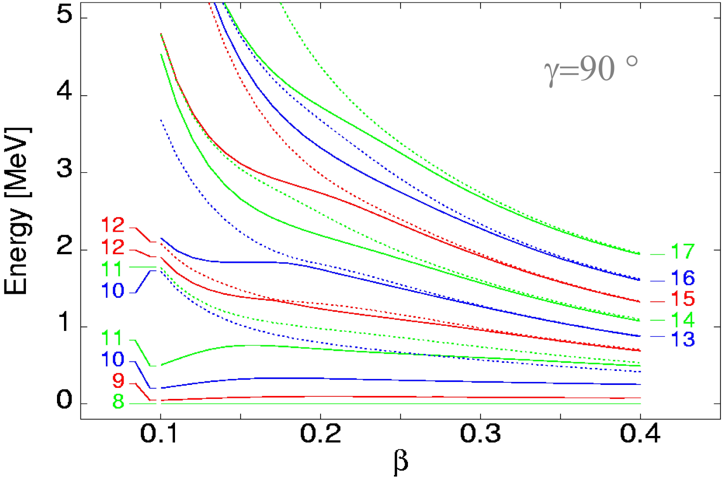

Geometry calculations

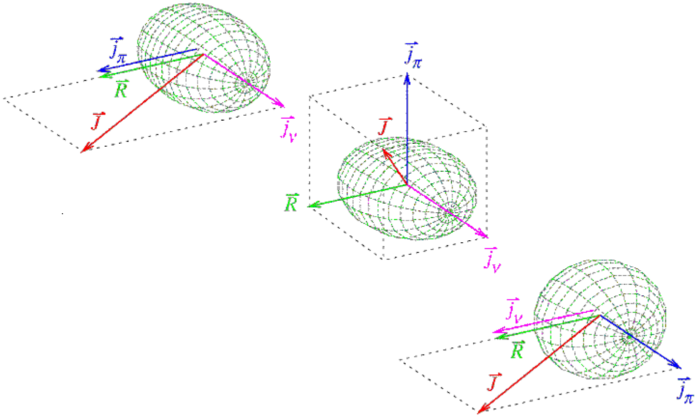

Geometry calculations

$$\sigma = (\vec{j}_\pi \times \vec{j}_\nu) \cdot \vec{R},$$

$$\langle I + | \sigma | I + \rangle = \langle I - | \sigma | I - \rangle = 0,$$

$$\tilde{\sigma} \equiv \frac{\langle IL | \sigma | IL \rangle}{\sqrt{\langle IL | j_\pi^2 | IL \rangle} \sqrt{\langle IL | j_\nu^2 | IL \rangle} \sqrt{\langle IL | R^2 | IL \rangle}}$$

Geometry calculations

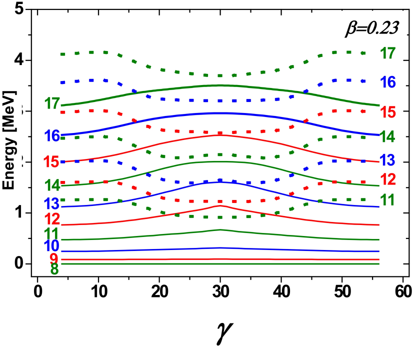

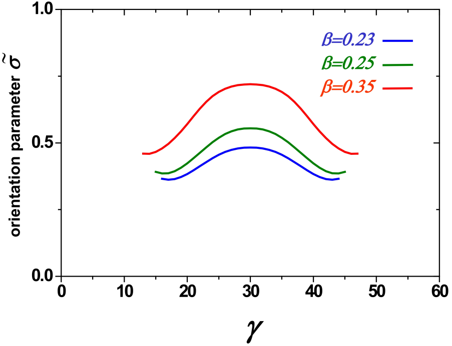

Fingerprints

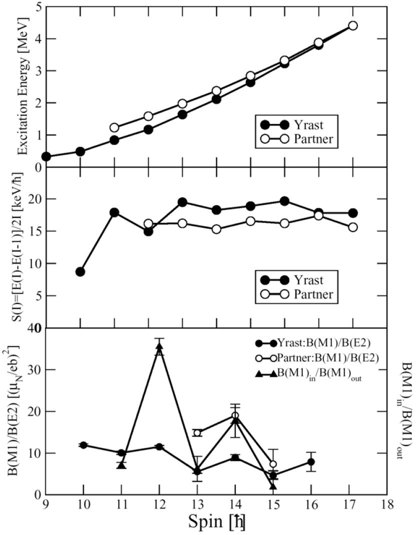

Fingerprints of chirality
in odd-odd nuclei

- near degenerate doublet $\Delta I=1$ bands for a range of spin I;
- $S(I)=[E(I)-E(I-1)]/2I$ independent of spin I;
- chiral symmetry restoration selection rules for M1 and E2 transitions vs. spin resulting in staggering of the absolute and relative transition strengths.

Simple yet untouched

Eugene P. Wigner
Group Theory,
Authors Preface

I like to recall his [von Laues] question as to which results derived in the present volume I considered most important. My answer was that the explanation of the concept of parity and the quantum theory of vector addition model appeared to me most significant. Since that time, I have come to agree with his answer that the recognition that almost all rules of spectroscopy follow from the symmetry of the problem is the most remarkable result.

Rotational invariance:

$|\Psi\rangle = |$ 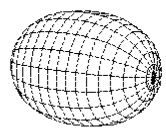 $\rangle$

$R(\omega)|\Psi\rangle = |$ 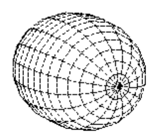 $\rangle$

$$R(\omega)|\Psi\rangle \neq |\Psi\rangle$$

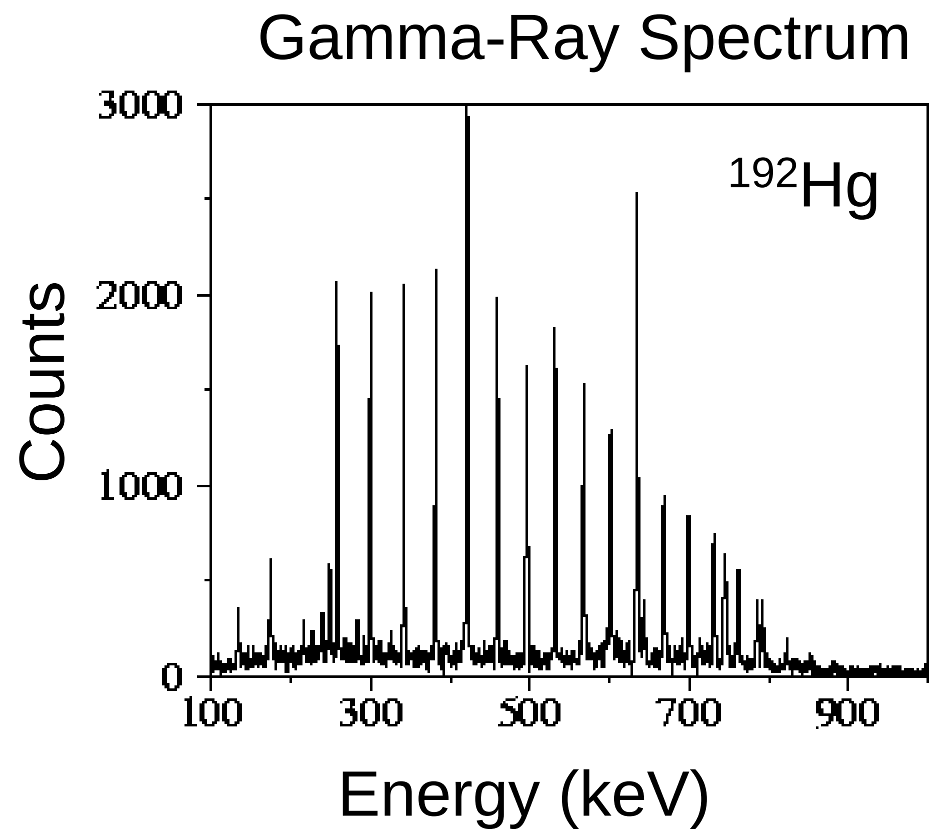

Space inversion invariance:

$$|\Psi\rangle = |$$ 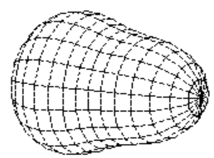 $$\rangle$$

$$P|\Psi\rangle = |$$ 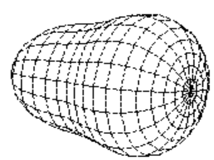 $$\rangle$$

$$P|\Psi\rangle \neq |\Psi\rangle$$

$^{222}_{88}$Ra

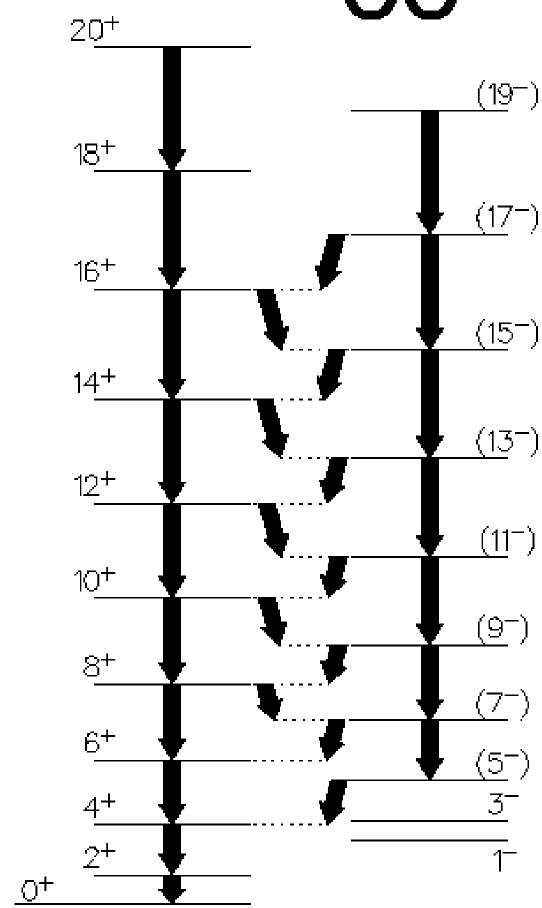

Space inversion vs time reversal:

Space inversion operation represented by $\mathbf{P}$ *is linear:*

$$\mathbf{P}\,(a|\psi_1\rangle + b|\psi_2\rangle) = a\,\mathbf{P}\,|\psi_1\rangle + b\,\mathbf{P}\,|\psi_2\rangle .$$

For the unitary operator $\mathbf{P}$ *:*

$$\mathbf{P}^2 = 1, \quad \mathbf{P}^{-1} = \mathbf{P} = \mathbf{P}^{\dagger} .$$

Eigenstates of $\mathbf{P}$ *with eigenvalues* $\pi=\pm 1$ *can be formed:*

$\mathbf{P}\,1/\sqrt{2}($ $|$ 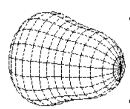 $\rangle + |$ 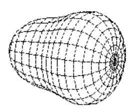 $\rangle$ $) = 1/\sqrt{2}($ $|$ 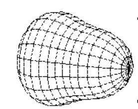 $\rangle + |$ 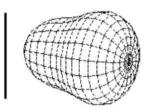 $\rangle$ $)$,

$\mathbf{P}\,1/\sqrt{2}($ $|$ 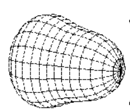 $\rangle - |$ 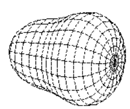 $\rangle$ $) = -1/\sqrt{2}($ $|$ 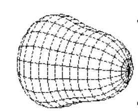 $\rangle - |$ 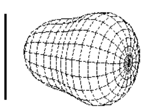 $\rangle$ $)$.

If $[\,\mathbf{P}\,,\,\mathbf{H}\,]=0$, *parity is a good quantum number for nuclear states.*

Space inversion vs time reversal:

Time reversal operation represented by $\mathbf{T}$ *is antilinear:*

$$\mathbf{T}(\boldsymbol{a}|\psi_1\rangle + \boldsymbol{b}|\psi_2\rangle) = \boldsymbol{a}^* \,\mathbf{T}\,|\psi_1\rangle + \boldsymbol{b}^* \,\mathbf{T}|\psi_2\rangle.$$

For the antiunitary operator $\mathbf{T}$ *:*

$$\mathbf{T}^2 = (-1)^{2I} = (-1)^A, \quad \mathbf{I}\text{-}\textit{spin}, \quad \mathbf{A}\text{-}\textit{number of fermions.}$$

Eigenstates of $\mathbf{T}$ *<u>can not</u> be defined.*

Despite $[\,\mathbf{T}\,,\,\mathbf{H}\,]=0$, *<u>there is no</u> quantum number associated with the time reversal symmetry.*

MICHIGAN STATE UNIVERSITY

For the nuclear hamiltonian which is invariant under time reversal the wave functions for physical states are required to be invariant under the operator $O = T\,R_y(\pi)$.

T denotes time reversal .

$R_y(\pi)$ denotes rotation by 180° around the axis perpendicular to the quantization axis.

With these definitions the O operator is a complex conjugation of expansion coefficients for wave functions in $|IM\rangle$ basis.

Since:

$$O\,|IM\rangle = |IM\rangle,$$

$$O\,\alpha|IM\rangle = \alpha^{*}|IM\rangle,$$

$$O^{2}\alpha|IM\rangle = \alpha|IM\rangle,$$

for an odd-odd nucleus there are two classes of states:

1) *planar states invariant under* O:

$$O\,|IP\rangle = |IP\rangle,$$

2) *right- and left- handed chiral states related by* O:

$$O\,|IR\rangle = |IL\rangle,$$

$$O\,|IL\rangle = |IR\rangle.$$

Simple yet untouched

$$O\,|I\,P\rangle = T\,R_y(\pi)\,|I\,P\rangle = |I\,P\rangle\,.$$

$T\,R_y(\pi)\Big|$ 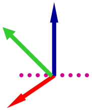 $\Big\rangle = T\Big|$ 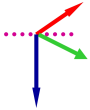 $\Big\rangle = \Big|$ 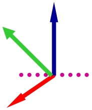 $\Big\rangle$

Simple yet untouched

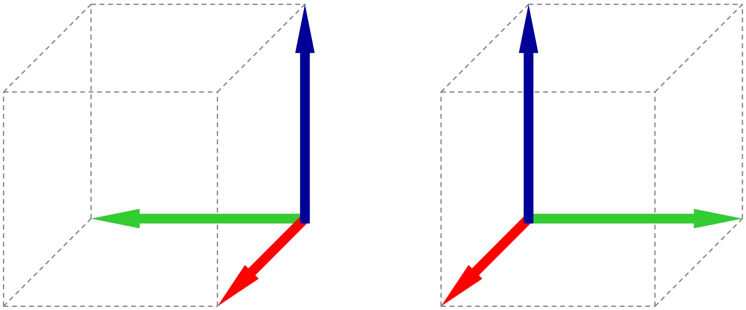

Simple yet untouched

$$O\,|I\,R\rangle = T\,R_y(\pi)\,|I\,R\rangle = |I\,L\rangle\,,$$

$$O\,|I\,L\rangle = T\,R_y(\pi)\,|I\,L\rangle = |I\,R\rangle\,.$$

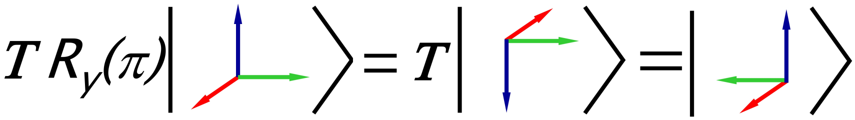

For $|I\,R\rangle$ and $|I\,L\rangle$ quantum mechanical analysis for a two level system directly applies.

(See for example ***Feynman lectures on Physics****.)*

Physical states invariant under O are:

$$|I+\rangle = \frac{1}{\sqrt{2}}(|IR\rangle + |IL\rangle),$$

$$|I-\rangle = \frac{i}{\sqrt{2}}(|IR\rangle - |IL\rangle),$$

For $\langle IR|H|IL\rangle = 0$,

if amplitude of the planar component is zero, then

$$\langle I+|H|I+\rangle = \langle I-|H|I-\rangle,$$

and physical states $|I+\rangle$, $|I-\rangle$ *are degenerate.*

If the planar component contributes significantly the degeneracy is lifted, the separation energy for the physical states $|I+\rangle$, $|I-\rangle$ *depends on the planar component amplitude.*

Molecular (geometric) chirality

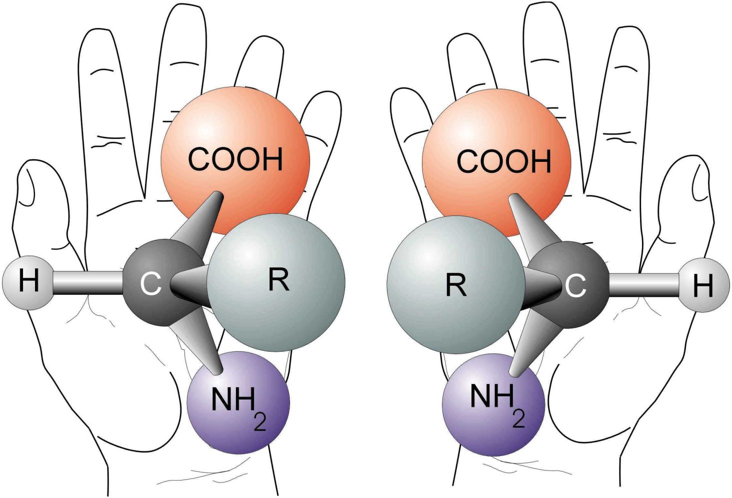

Chirality unique to atomic nuclei

Atomic nuclei are the only systems which can provide two single-particle angular momenta components needed for angular-momentum chirality.

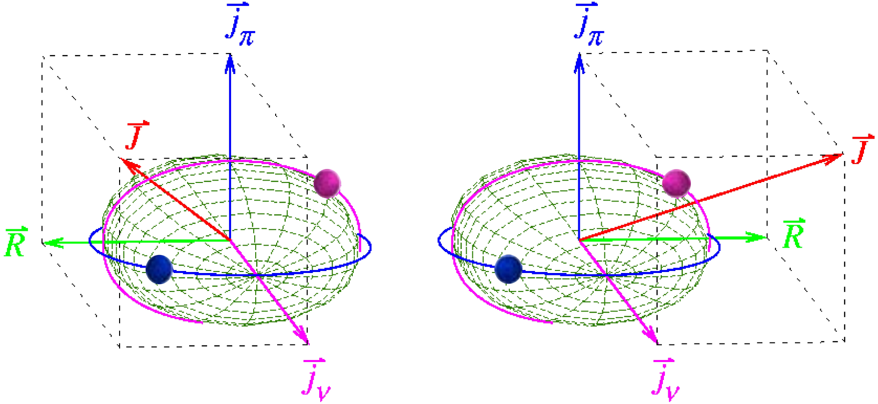

Consistent with many models

For triaxial odd-odd nuclei

Chirality =

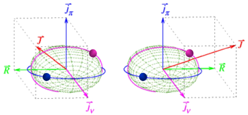

Nilsson model +

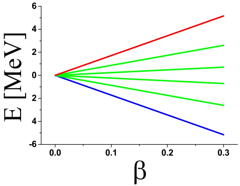

irrotational flow
moment of inertia

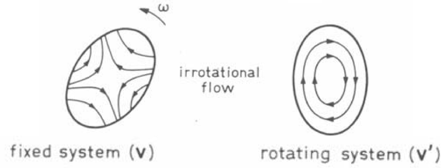

Consistent with many models

- Particle-rotor
- Tilted Cranked Shell Model
- Interacting Boson Fermion-Fermion
- Cranked Hartree-Fock-Bogolubov

Signature of static triaxiality

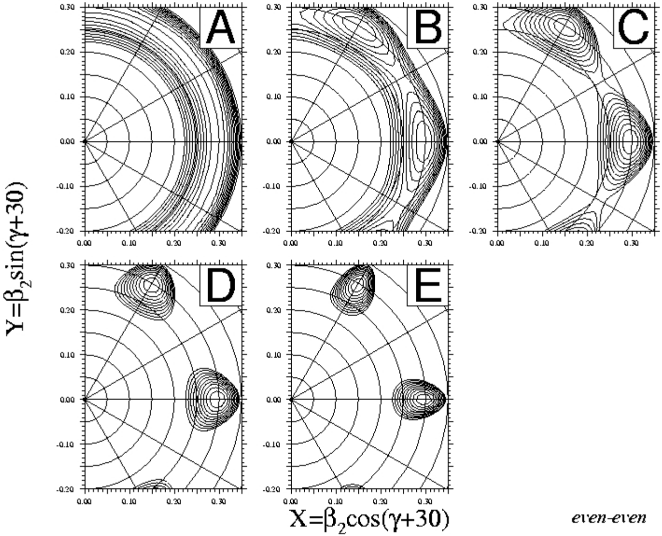

Signature of static triaxiality

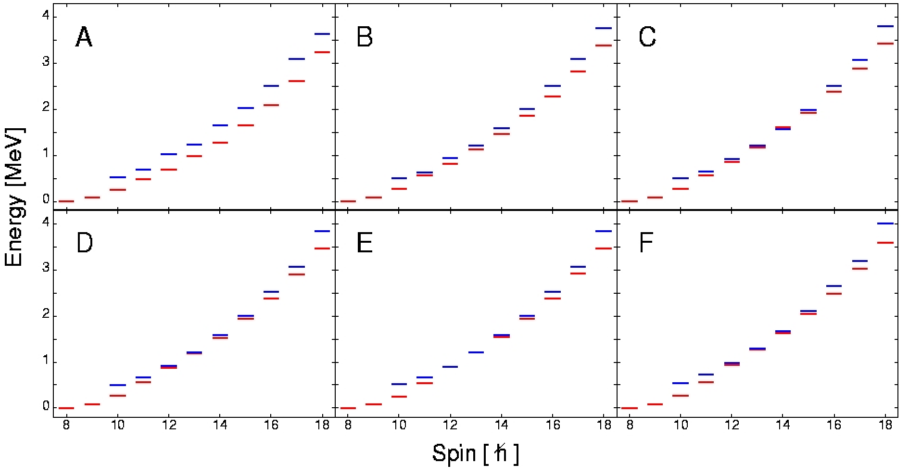

Signature of irrotational flow

$$J_k^{irr.} = J_0 \frac{4}{3} \sin^2\left(\gamma - \frac{2}{3}\pi k\right) \qquad J_k^{rig.} = J_0\left(1 + \sqrt{\frac{5}{4\pi}}\beta\cos\left(\gamma - \frac{2}{3}\pi k\right)\right)$$

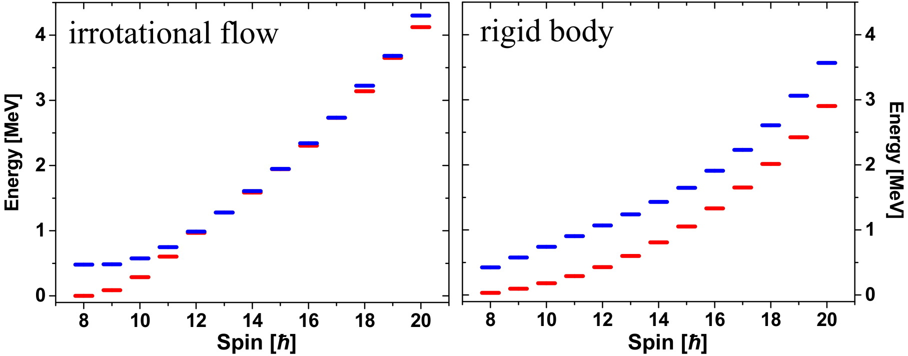

A model for core-particle-hole coupling in the intrinsic reference frame:

based on a transformation from the laboratory (inertial) into the intrinsic, body fixed (noninertial), reference frame,

the results of the calculation do not depend on how the reference frame is chosen,

the convenience to carry out the calculations, however, depends on that choice significantly.

For irrotational flow moment of inertia there are two special cases for which two out of three moments are equal:

axial symmetry

for $\gamma=0^o$ *(prolate shapes)*

$J_s=J_i=J_0 \quad J_l=0$

for $\gamma=60^o$ *(oblate shapes)*

$J_l=J_i=J_0 \quad J_s=0$

triaxiality

for $\gamma=30^o$ *(triaxial shapes)*

$J_l=J_s=J_0 \quad J_i=4J_0.$

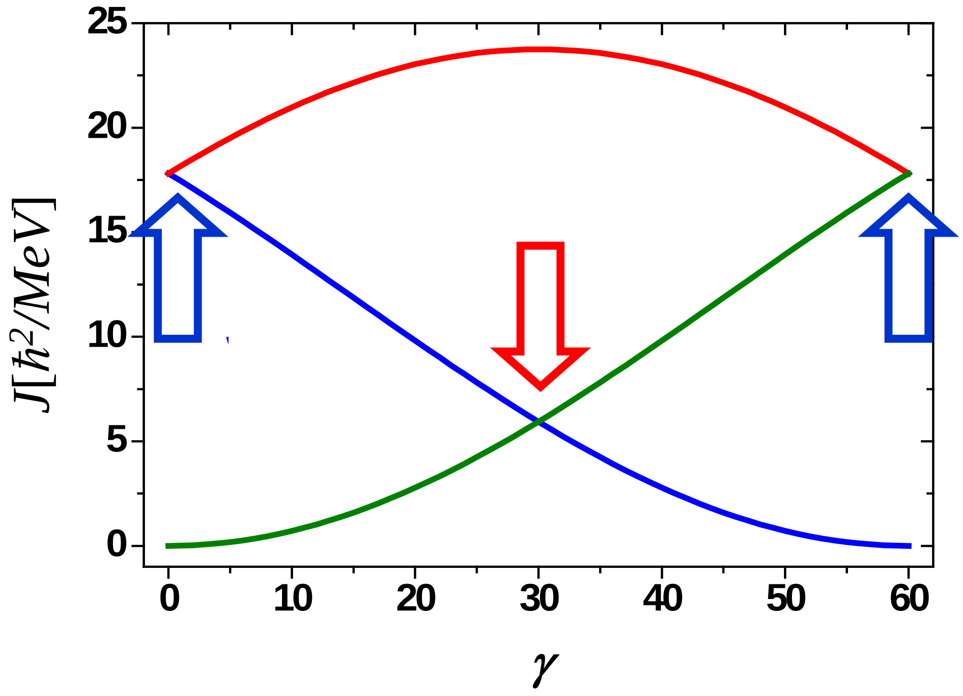

For triaxial shapes at $\gamma=30^o$ *the rotor hamiltonian has a very similar structure to the hamiltonian for axially symmetric shapes.*

The intermediate axis becomes an effective symmetry axis.

Quantum mechanics of an axially symmetric rotor:

MICHIGAN STATE UNIVERSITY

the symmetry axis is a convenient quantization axis in the intrinsic reference frame,

collective rotation around the symmetry axis is forbidden and $J_3 \equiv 0$, the axis of rotation is perpendicular to the symmetry axis, and the only value allowed for R_3 is $K=0$,

$$H = \hbar^2/2 \cdot \Sigma_i R_i^2/J_i = \hbar^2/2J_0 \cdot (R^2 - R_3^2)$$

$$E = \hbar^2/2J_0 \cdot [R(R+1) - K^2] = \hbar^2/2J_0 \cdot R(R+1).$$

Quantum mechanics of a triaxial rotor:

the effective symmetry axis (the intermediate axis) is a convenient quantization axis in the intrinsic reference frame,

for the Bohr parameterization intermediate axis coincides with the quantization axis in the intrinsic reference frame for $\gamma=90^o$.

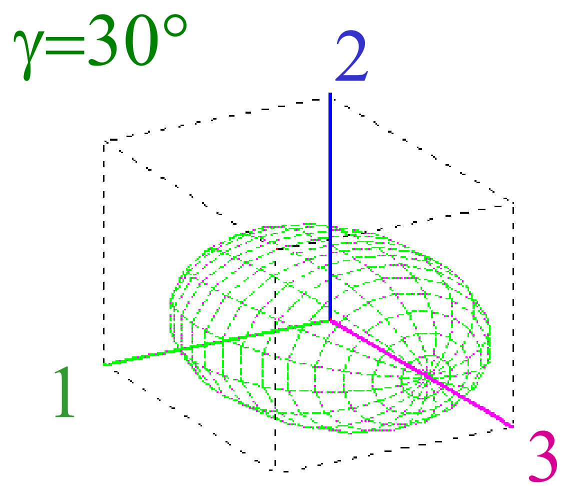

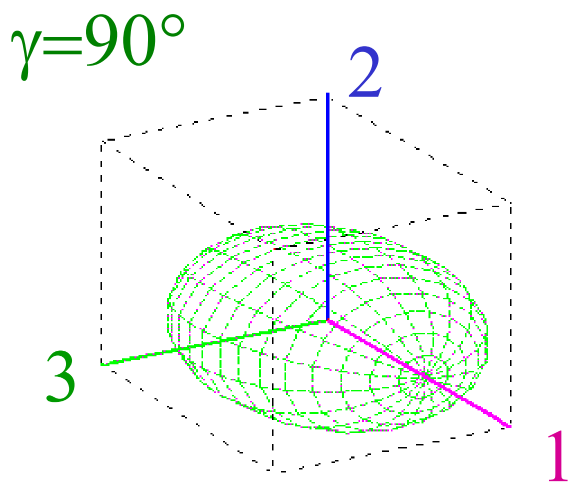

Quantum mechanics of a triaxial rotor:

MICHIGAN STATE UNIVERSITY

the effective symmetry axis (the intermediate axis) is a convenient quantization axis in the intrinsic reference frame, for the Bohr parameterization intermediate axis coincides with the quantization axis in the intrinsic reference frame for $\gamma=90^o$,

since J_3 is the largest of the moments of inertia, collective rotation around the quantization axis is favored,

for yrast states the axis of rotation is oriented along the quantization axis and R_3 has the maximum value $K=R$,

$$H=\hbar^2/2\cdot\Sigma_i R_i^2/J_i = \hbar^2/2J_0\cdot(R^2-3/4\cdot R_3^2), \quad E=\hbar^2/2J_0\cdot[R(R+1)-3/4\cdot K^2].$$

Quadrupole deformed shape is invariant under rotation by 180° about any of the principal axes:

rotation operators:

$R_1(\pi), R_2(\pi), R_3(\pi)$
in the intrinsic reference frame together with an identity operator form the D_2 symmetry group,

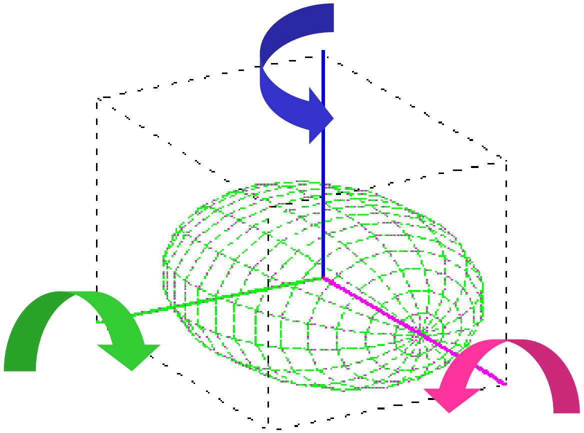

wave functions invariant under the D_2 symmetry given by:

$$|RMK\rangle = 1/\sqrt{2}\,[D^R_{MK}(\omega) + (-1)^R \cdot D^R_{M-K}(\omega)]$$

with only even K allowed, form a basis for diagonalization of the rotor hamiltonian.

Unique parity $h_{11/2}$ state in quadrupole-deformed triaxial potential.

$$H = H_{SM} + H_{def}$$

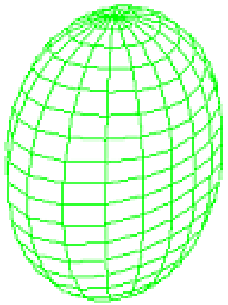

Triaxial shape for β = 0.3, γ = 30°.

$$H_{def} = k\beta\,[\,\cos(\gamma)Y_{20}(\theta,\phi) + 1/\sqrt{2}\sin(\gamma)\{Y_{22}(\theta,\phi) + Y_{2-2}(\theta,\phi)\}]$$

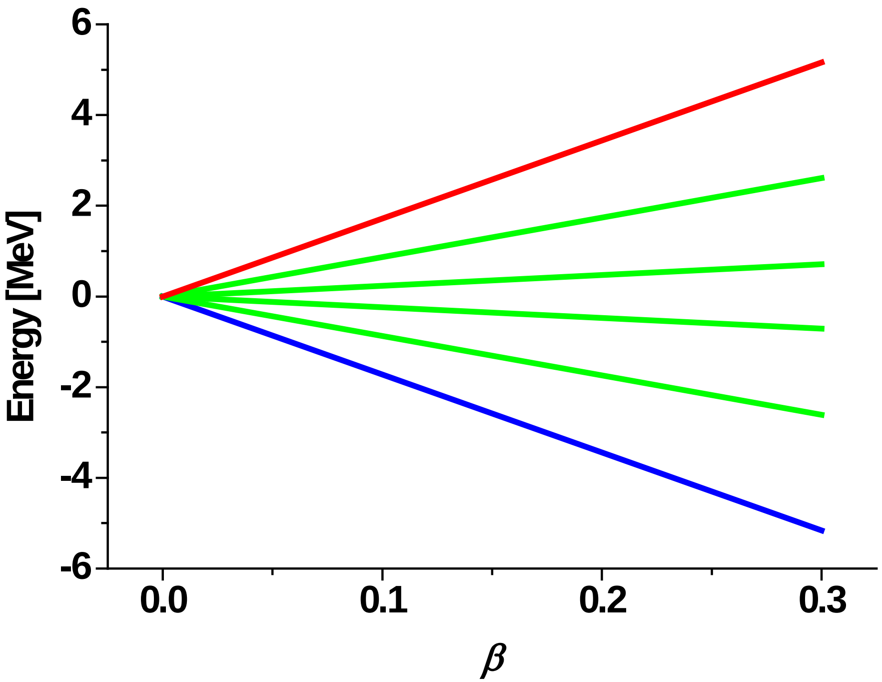

$\langle j_s \rangle = 0.00 \quad \langle \sigma_s \rangle = 1.36$
$\langle j_i \rangle = 0.00 \quad \langle \sigma_i \rangle = 2.01$
$\langle j_l \rangle = \pm 5.46 \quad \langle \sigma_l \rangle = 0.30$

$\langle j_s \rangle = \pm 5.46 \quad \langle \sigma_s \rangle = 0.30$
$\langle j_i \rangle = 0.00 \quad \langle \sigma_i \rangle = 2.01$
$\langle j_l \rangle = 0.00 \quad \langle \sigma_l \rangle = 1.36$

D_2 symmetry and γ value

For $\gamma' = \gamma + 60°$ corresponding triaxial shapes are the same; however, labeling of principal axes changes.

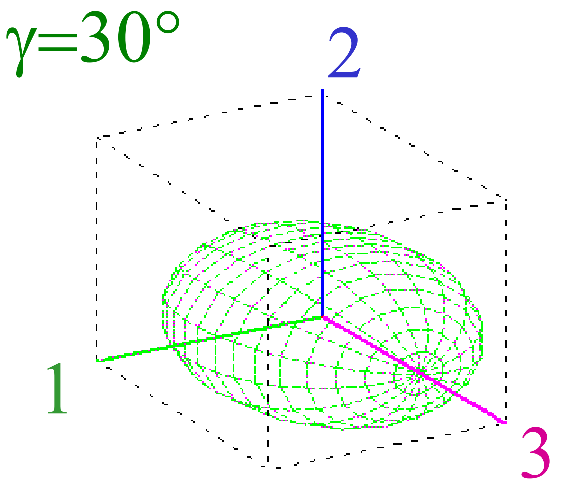

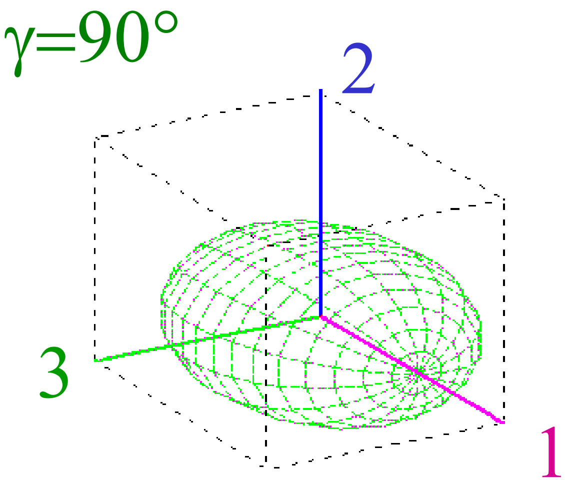

Why should we chose $\gamma = 90°$?

- Intermediate axis becomes quantization axis.

- Single particle hamiltonian simplifies, since

  $\cos(\gamma) = 0$, $\sin(\gamma) = 1$:

$$H_{def} = k\beta/\sqrt{2}\{Y_{22}(\theta,\phi) + Y_{2-2}(\theta,\phi)\}.$$

- For a single j-shell H_{def} can be expressed using j_+, j_- or j_x, j_y angular momentum operators:

$$H_{def} \propto k\beta/\sqrt{2}\{j_x^2 - j_y^2\} \propto k\beta/\sqrt{2}\{j_+^2 + j_-^2\}.$$

Semi classical analysis for single-particle hamiltonian with $\gamma=90^{\circ}$.

$$j^2 = j_x^2 + j_y^2 + j_z^2 \qquad E - E_F = \kappa\,(j_x^2 - j_y^2)$$

$E > E_F$

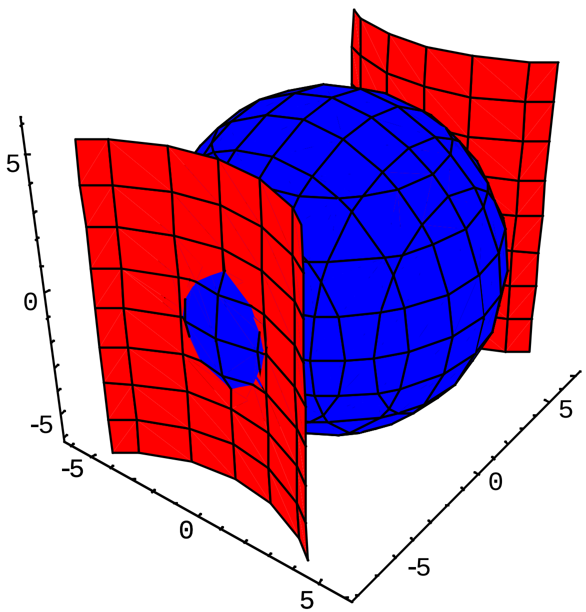

$E < E_F$

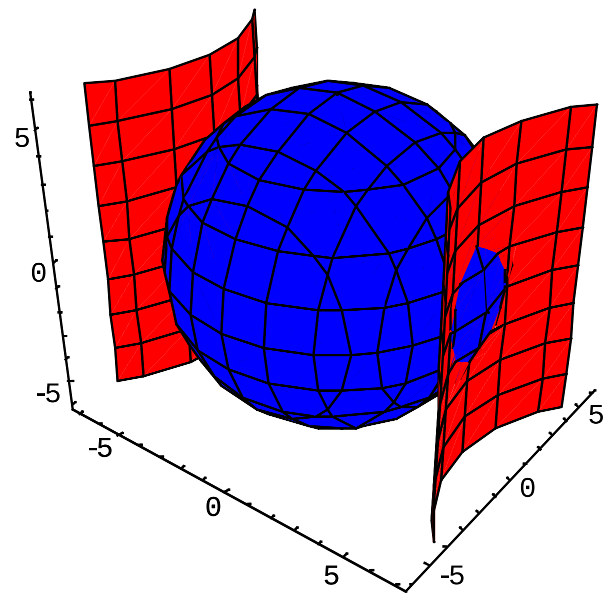

Symmetry of triaxial quadrupole-deformed potential.

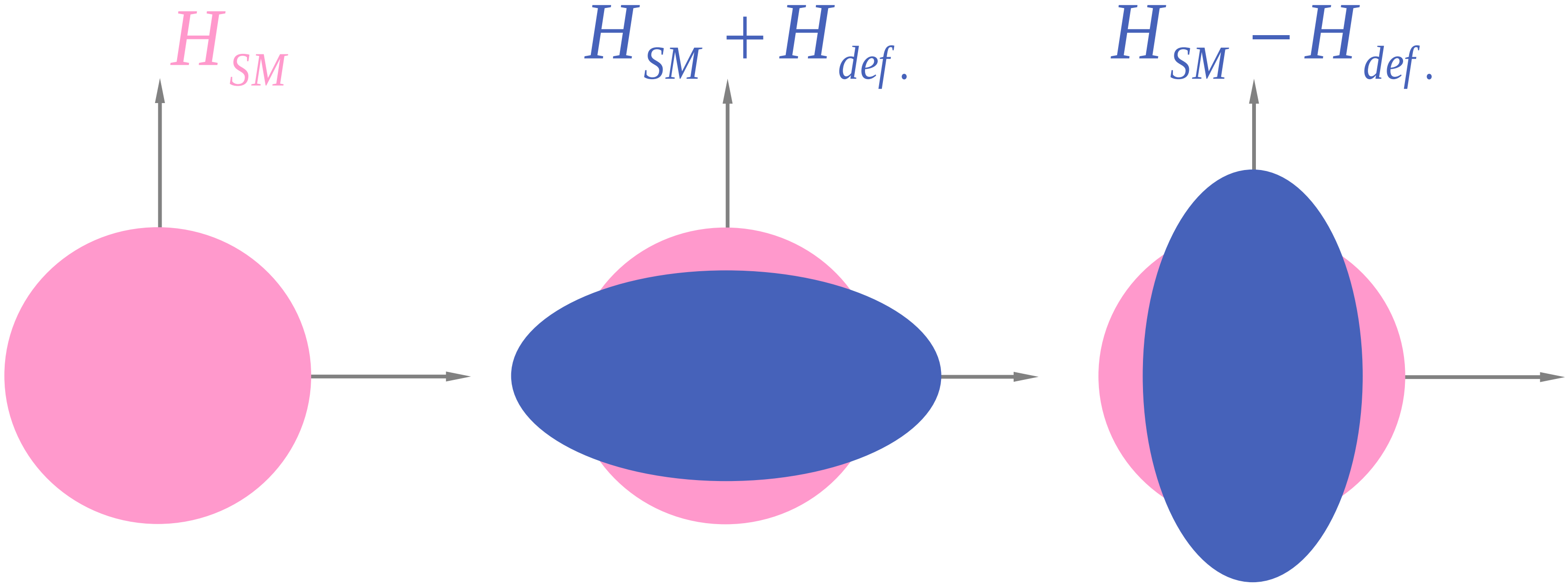

$$R_i(\pi/2) H_{def.} R_i^{-1}(\pi/2) = -H_{def.}$$

$$|\Psi'\rangle = R_i(\pi/2)|\Psi\rangle$$

$$H_{def.}|\Psi\rangle = \varepsilon|\Psi\rangle \Rightarrow H_{def.}|\Psi'\rangle = -\varepsilon|\Psi'\rangle$$

Quantum mechanics of a triaxial rotor with proton and neutron coupled:

the intermediate, effective symmetry axis is a convenient quantization axis in the intrinsic reference frame ($\gamma=90^o$),

wave functions invariant under the D_2 *symmetry are:*

$$|IMK\, j_\pi \Omega_\pi\, j_\nu \Omega_\nu \rangle = 1/\sqrt{2}[D^I_{MK}(\omega)\, |j_\pi \Omega_\pi\rangle\, |j_\nu \Omega_\nu\rangle + (-1)^{I-j_\pi-j_\nu} \cdot D^I_{M-K}(\omega)\, |j_\pi -\Omega_\pi\rangle\, |j_\nu -\Omega_\nu\rangle\,]$$

with only even $K-\Omega_\pi-\Omega_\nu$ *allowed,*

these wavefunctions form a basis for diagonalization of the single particle plus rotor hamiltonian: $H=H_{sp}+H_{rot}$

Two step diagonalization of the single particle plus rotor hamiltonian at $\gamma=90^o$:

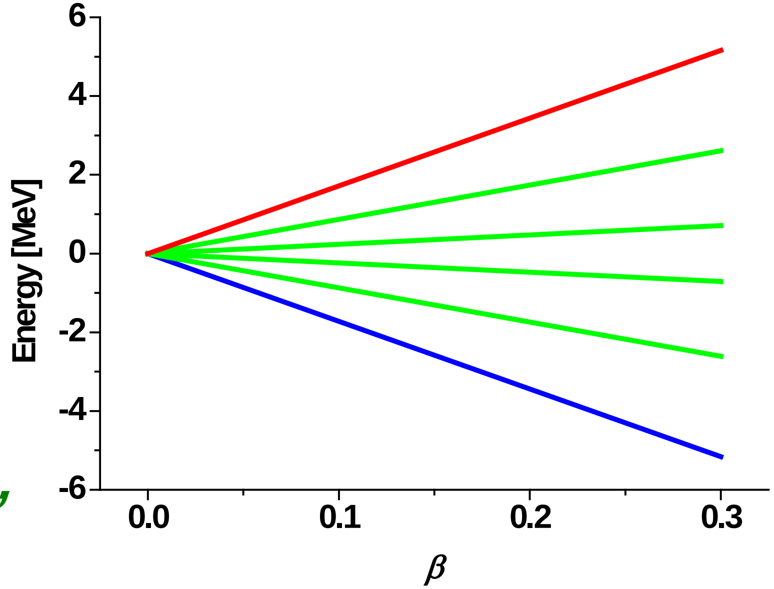

single particle hamiltonian

$$H_{sp}=k\beta/\sqrt{2}\cdot[Y_{22}(\theta,\varphi)+Y_{2-2}(\theta,\varphi)]$$

is diagonalized in the first step,

resulting wave functions are used in the second step for diagonalization of the full hamiltonian,

$$H_{rot}=\hbar^2/2J_0\cdot[I^2+j_\pi^2+j_\nu^2-3/4\cdot(I_3^2+j_{\pi 3}^2+j_{\nu 3}^2) -I_+(j_{\pi -}+j_{\nu -})-I_-(j_{\pi +}+j_{\nu +})-1/2\cdot I_3(j_{\pi 3}+j_{\nu 3}) +j_{\pi +}j_{\nu -}+j_{\pi -}j_{\nu +}+1/2\,j_{\pi 3}\,j_{\nu 3}].$$

The doublet states result from diagonalization of the single particle hamiltonian in the first step,

<u>except for the states with $K=0$.</u>

The doublet states are split when the rotor part is included in diagonalization in the second step.

The predicted splitting depend on the coupling strength of the single particle hamiltonian :

$k\beta = 206/A^{1/3}\beta$ *which increases linearly with deformation,*

as compared to the coupling strength of the rotor hamiltonian:

$\hbar^2/2J_0 = \hbar^2/2B\beta^2$ *which decreases as* $1/\beta^2$.

The predicted splitting is small at large β.

$\pi h_{11/2} \nu h_{11/2}$ particle-hole coupling at $\gamma=90°$ as a function of β with the single particle coupling strength constant.

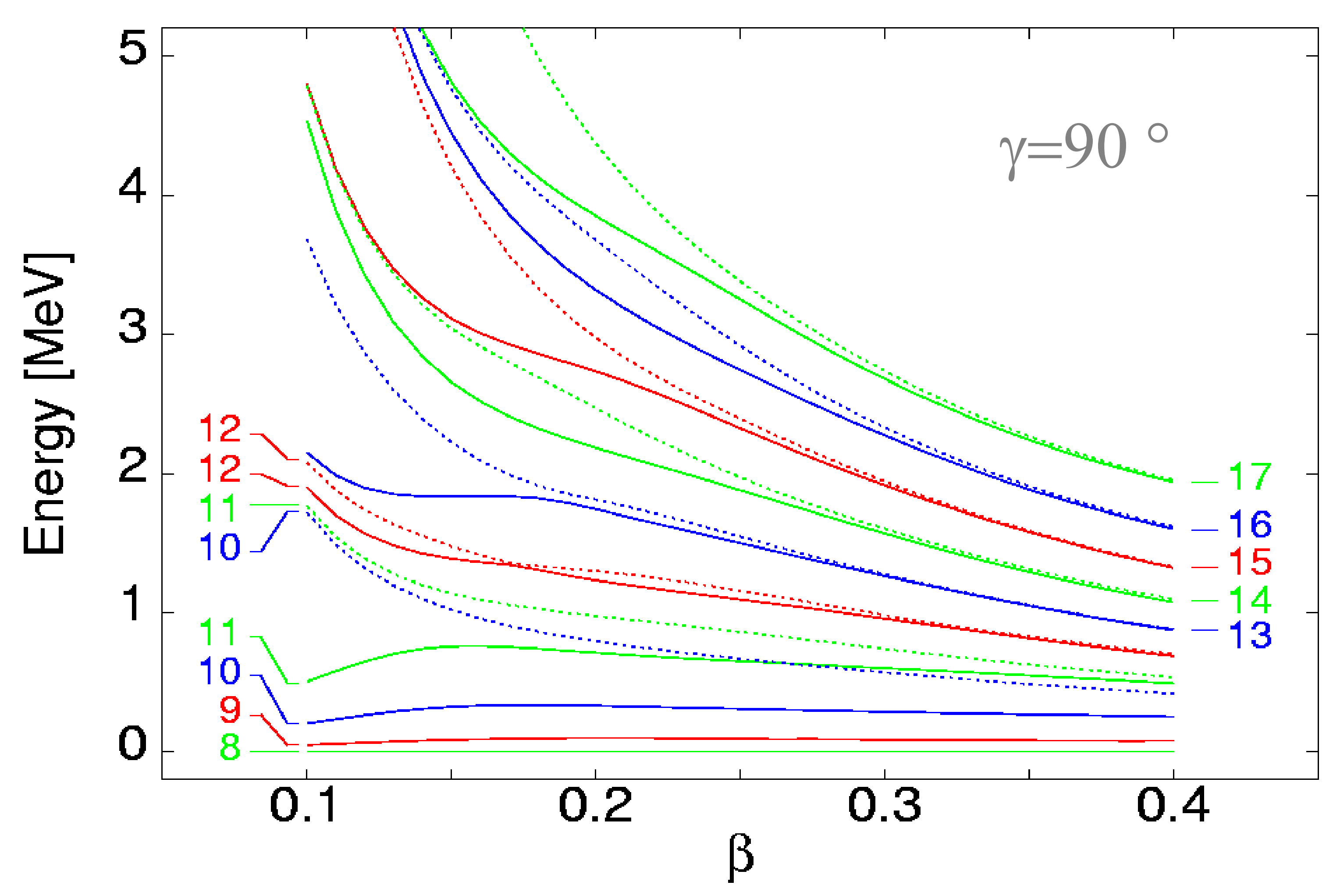

Model predicts an existence of chiral partner bands for deformed ($\beta \sim 0.3$) *triaxial nuclei* ($\gamma = 90^{o}$ *or* 30^{o}).

Calculations in the intrinsic reference frame results in very simple wave functions with relatively small number (~10) of dominating components.

The simplicity of the wave function in the intrinsic reference frame provides an effective way to examine an underlying physics. In particular, the $|I\,R\rangle$ *and* $|I\,L\rangle$ *wave functions for the right- and left-handed system can be extracted (but note the* $K=0$ *component).*

The wavefunction in the intrinsic reference frame $\beta=0.3$, $\gamma=90^o$, the distribution for single particle proton states.

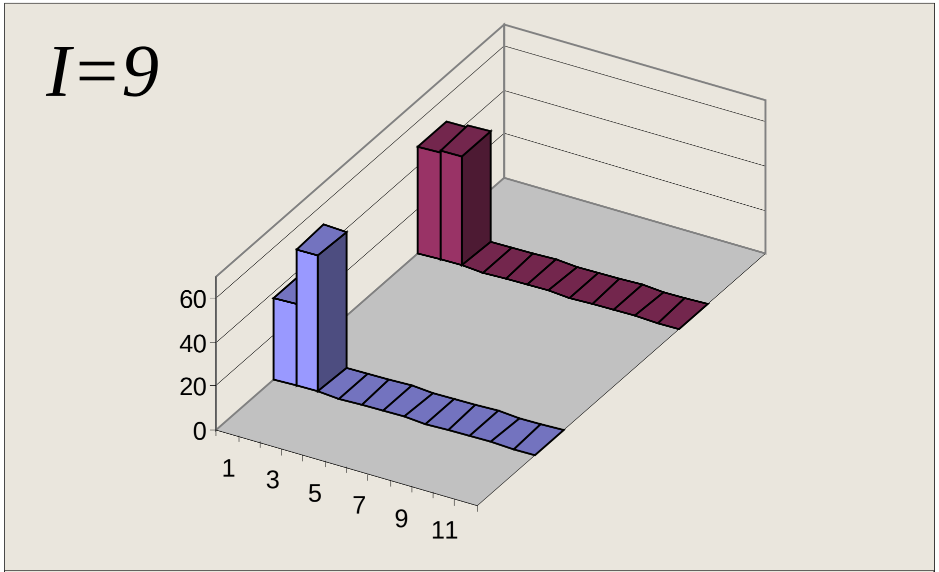

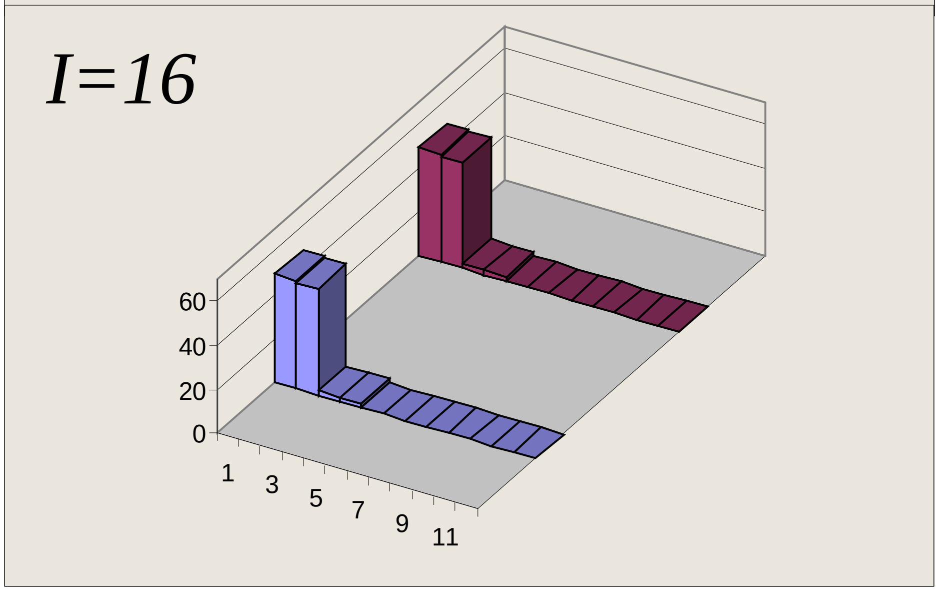

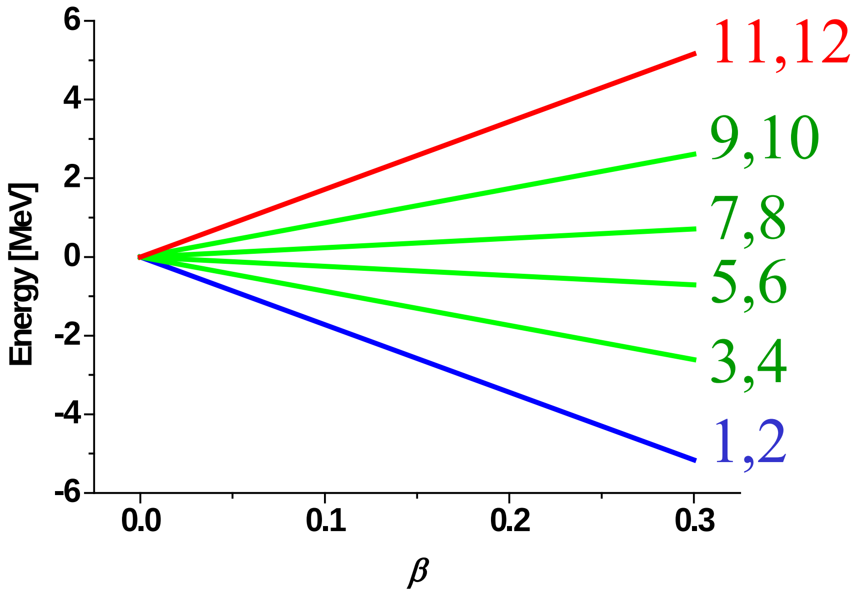

The wavefunction in the intrinsic reference frame $\beta=0.3, \gamma=90^o$, the distribution for single particle neutron states.

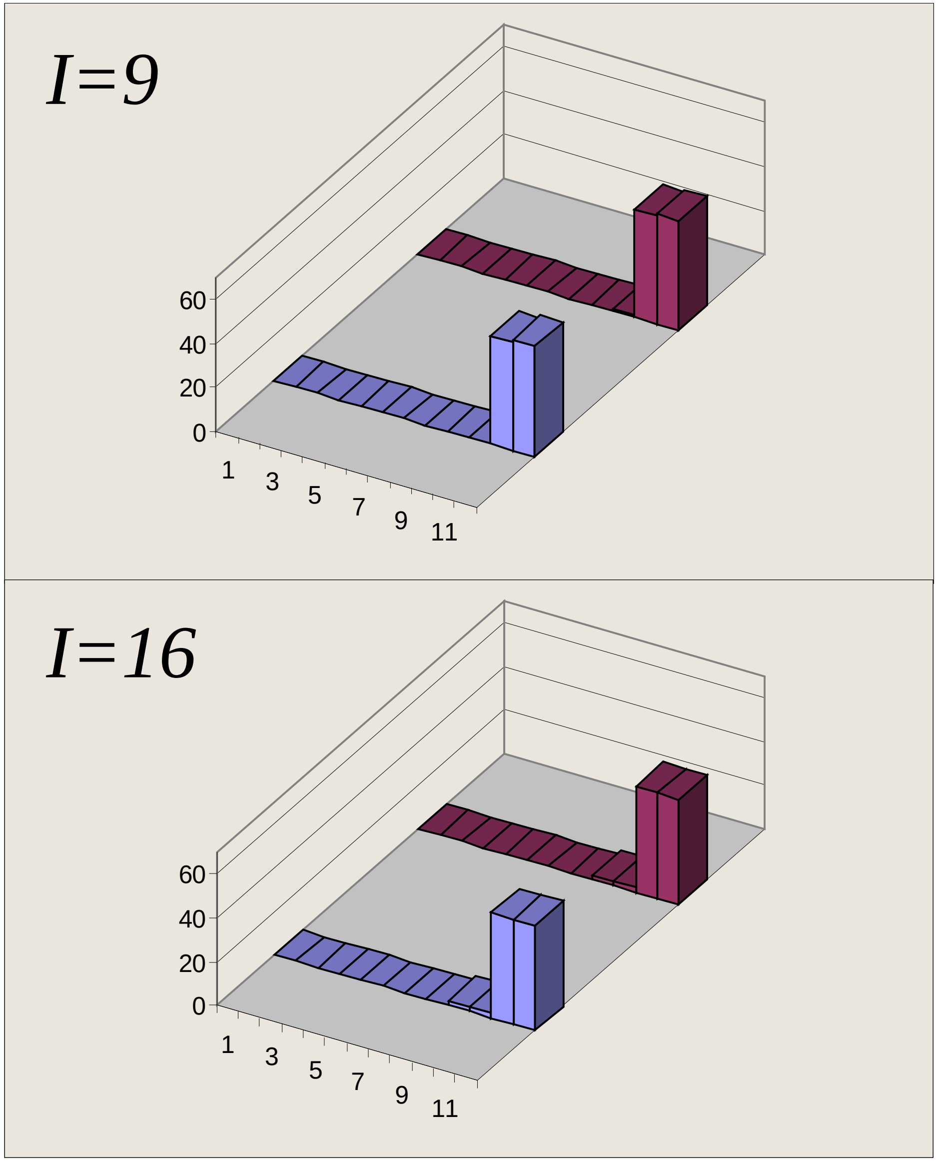

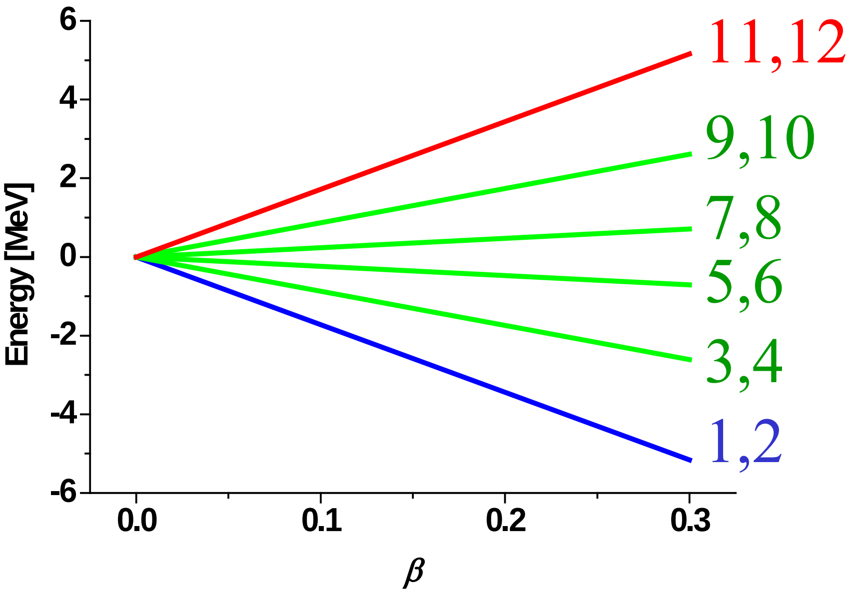

The wavefunction in the intrinsic reference frame $\beta=0.3$, $\gamma=90^o$, *the distribution for the rotor* K *states.*

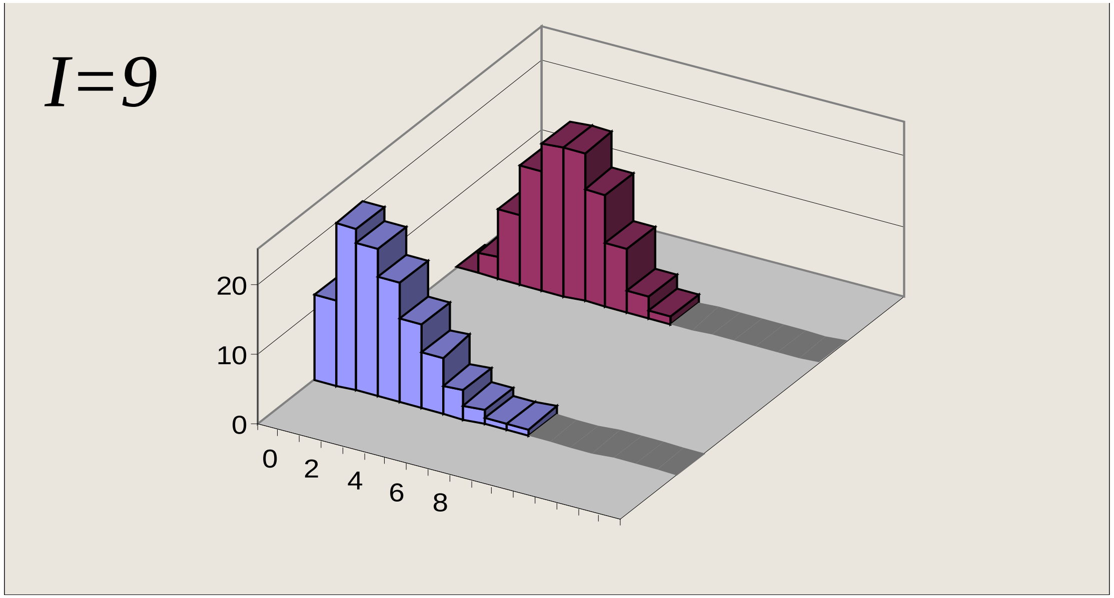

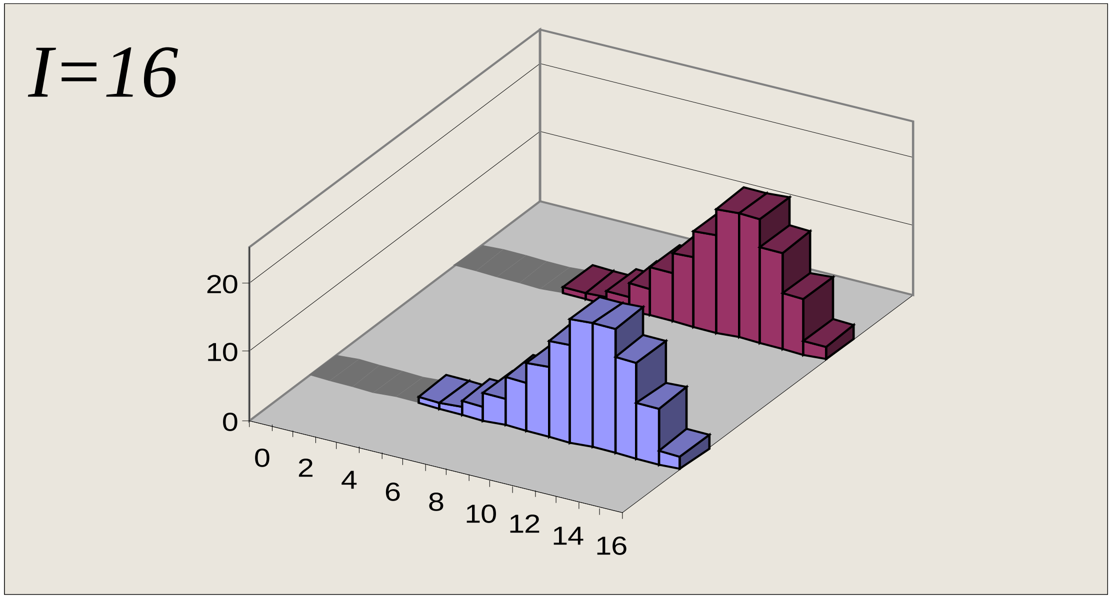

The role of K=0 components:

the basis states with K=0 are the only states for which the right- and the left-handed wavefunctions <u>can not</u> be defined,

states with K=0 are “planar”, while states with K≠0 are “chiral”,

relatively large amplitudes for the “planar” components result in separation of doublet states at low spin.

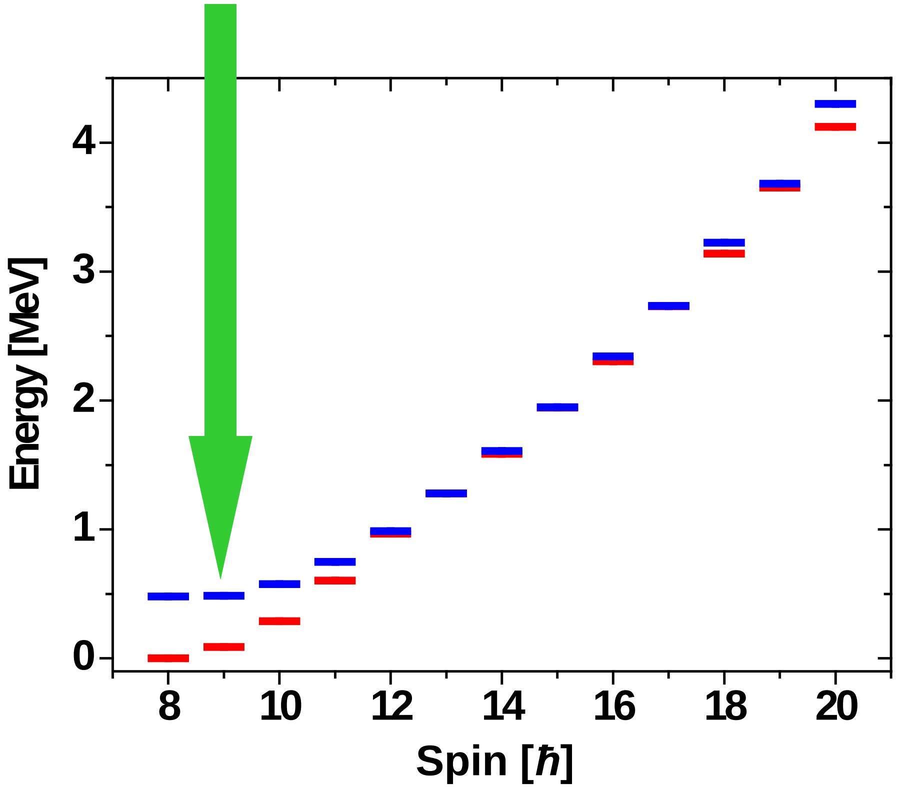

Calculated Level Scheme

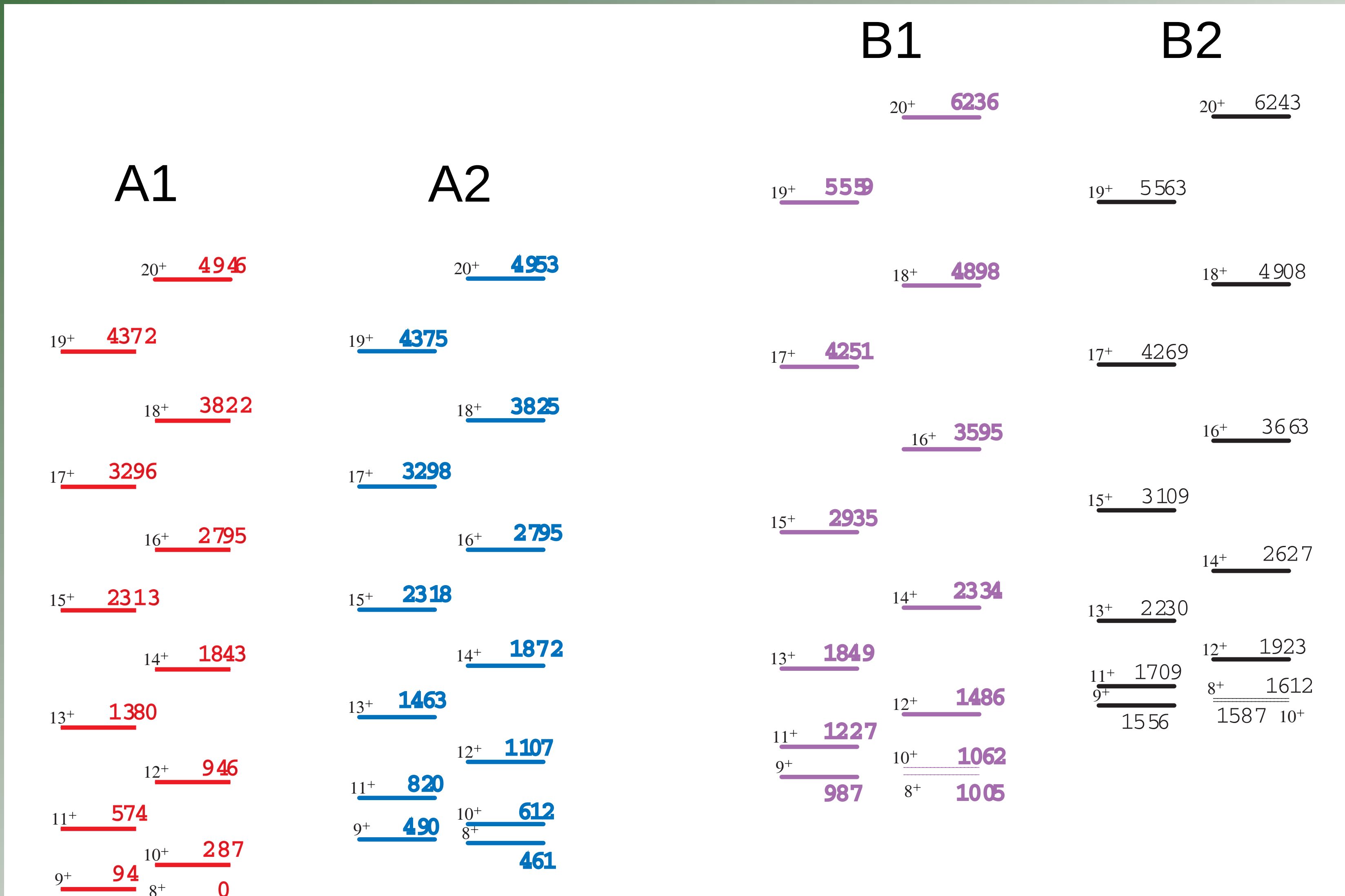

Energy vs Spin: pairs of degenerate bands

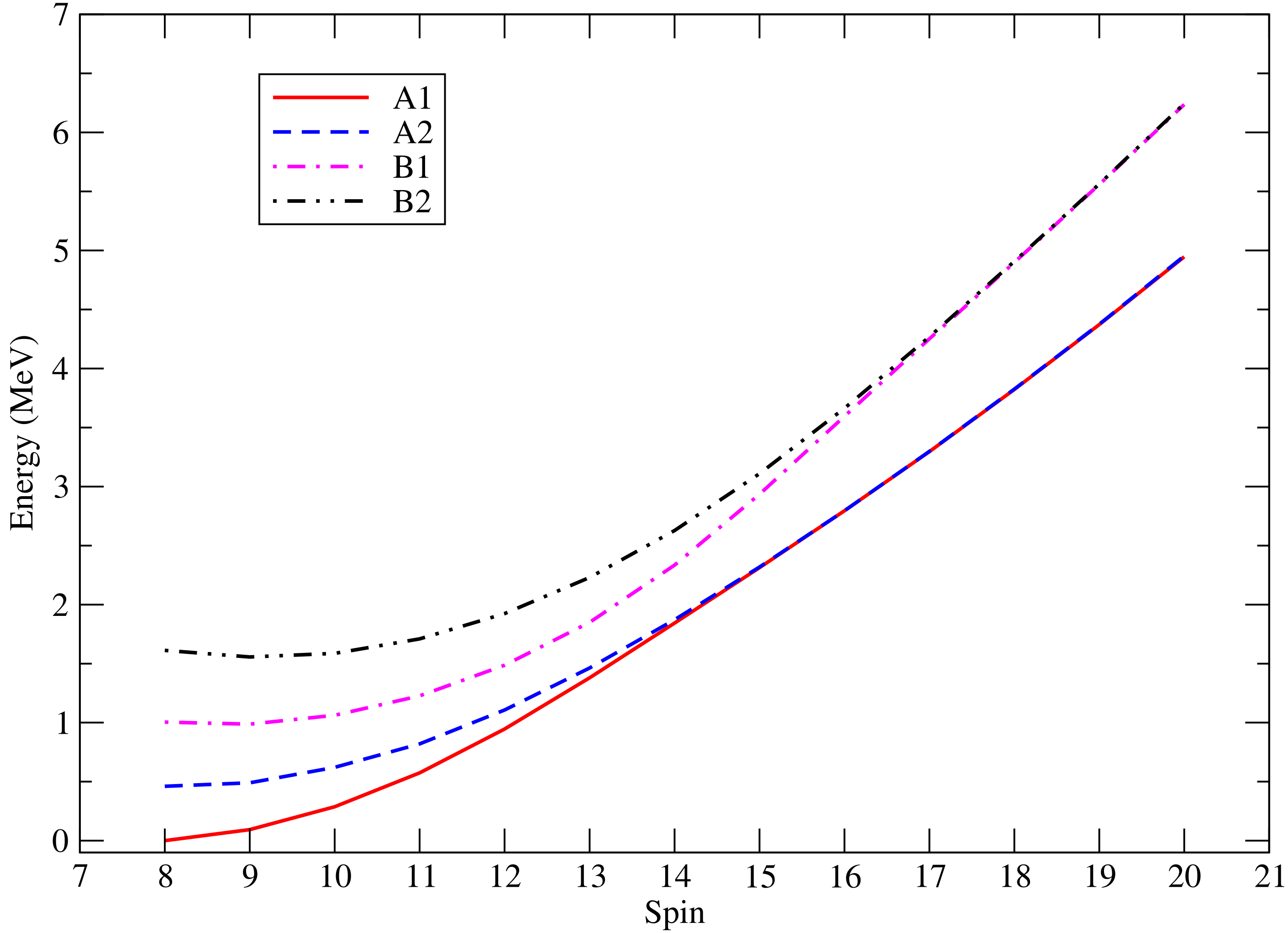

Selection rules for E-M transitions

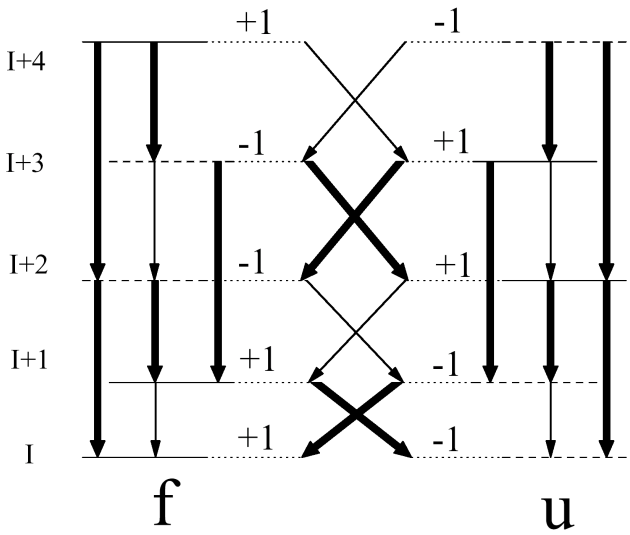

Doublet bands in many mass regions

A∼130				A ∼105			
Nucleus	s.p. config.		*E.M.*	Nucleus	s.p. config.		*E.M.*
^{140}Eu[3]	$\pi h_{11/2}\nu h_{11/2}$	o-o		^{106}Ag[18]	$\pi g_{9/2}\nu h_{11/2}$	o-o	
^{138}Eu[4]	$\pi h_{11/2}\nu h_{11/2}$	o-o		^{105}Ag[19]	$\pi g_{9/2}\nu {h_{11/2}}^2$	o-A	
^{136}Pm[5]	$\pi h_{11/2}\nu h_{11/2}$	o-o		^{106}Rh[20]	$\pi g_{9/2}\nu h_{11/2}$	o-o	
^{136}Nd[6]	$\pi h_{11/2}(d_{5/2},g_{7/2})\nu {h_{11/2}}^2$	e-e		^{105}Rh[21]	$\pi g_{9/2}\nu {h_{11/2}}^2$	o-A	
^{135}Nd[7]	$\pi {h_{11/2}}^2\nu h_{11/2}$	o-A	[29]	^{104}Rh[22]	$\pi g_{9/2}\nu h_{11/2}$	o-o	[33]
^{134}La[8]	$\pi h_{11/2}\nu h_{11/2}$	o-o		^{103}Rh[23]	$\pi g_{9/2}\nu {h_{11/2}}^2$	o-A	[33]
^{132}La[9]	$\pi h_{11/2}\nu h_{11/2}$	o-o	[30]	^{102}Rh[23]	$\pi g_{9/2}\nu h_{11/2}$	o-o	
^{130}La[10]	$\pi h_{11/2}\nu h_{11/2}$	o-o		^{112}Ru[24]	$\nu h_{11/2}(d_{5/2},g_{7/2})$	e-e	
^{134}Pr[11]	$\pi h_{11/2}\nu h_{11/2}$	o-o	[31]	^{110}Ru[24]	$\nu h_{11/2}(d_{5/2},g_{7/2})$	e-e	
^{132}Pr[10]	$\pi h_{11/2}\nu h_{11/2}$	o-o		^{108}Ru[24]	$\nu h_{11/2}(d_{5/2},g_{7/2})$	e-e	
^{128}Pr[12]	$\pi h_{11/2}\nu h_{11/2}$	o-o		^{100}Tc[25]	$\pi g_{9/2}\nu h_{11/2}$	o-o	
^{132}Cs[13]	$\pi h_{11/2}\nu h_{11/2}$	o-o		^{106}Mo[26]	$\nu h_{11/2}(d_{5/2},g_{7/2})$	e-e	
^{130}Cs[14]	$\pi h_{11/2}\nu h_{11/2}$	o-o	[32]				
^{128}Cs[15]	$\pi h_{11/2}\nu h_{11/2}$	o-o	[30]				
^{126}Cs[16]	$\pi h_{11/2}\nu h_{11/2}$	o-o					
^{124}Cs[17]	$\pi h_{11/2}\nu h_{11/2}$	o-o					
A ∼190				A∼80**			
Nucleus	s.p. config.		*E.M.*	Nucleus	s.p. config.		*E.M.*
^{188}Ir†[27]	$\pi h_{9/2}\nu i_{13/2}$	o-o			$\pi g_{9/2}\nu g_{9/2}$	o-o	
^{198}Tl[28]	$\pi h_{9/2}\nu i_{13/2}$	o-o			$\pi {g_{9/2}}^2\nu g_{9/2}$	o-A	

Odd-mass systems

^{105}Rh

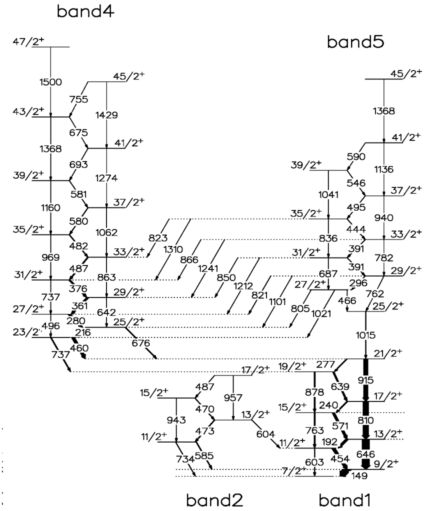

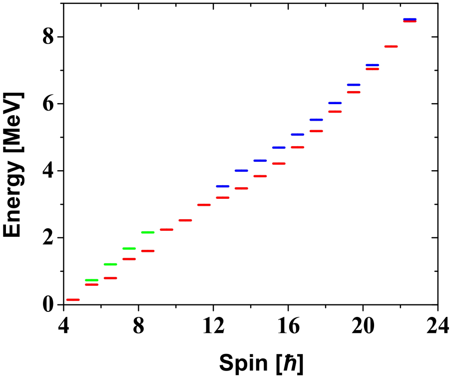

Phonon-like excitation structure

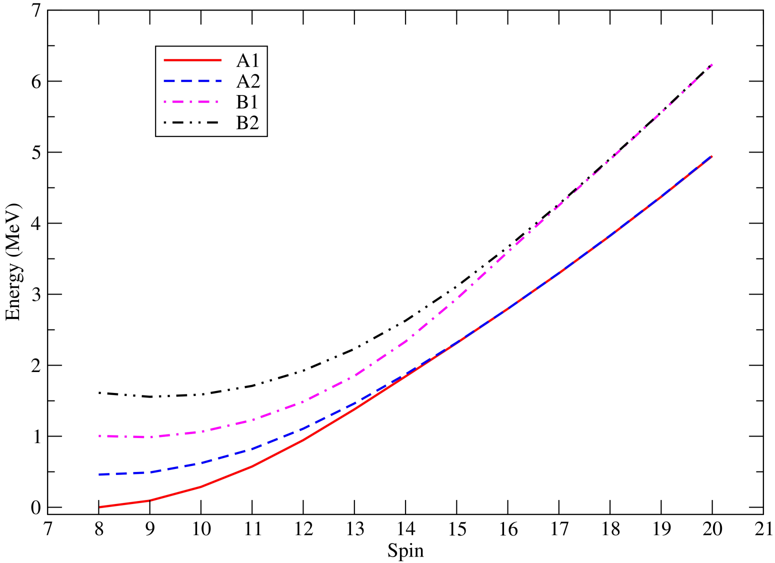

Issues with transition rates: ^{134}Pr

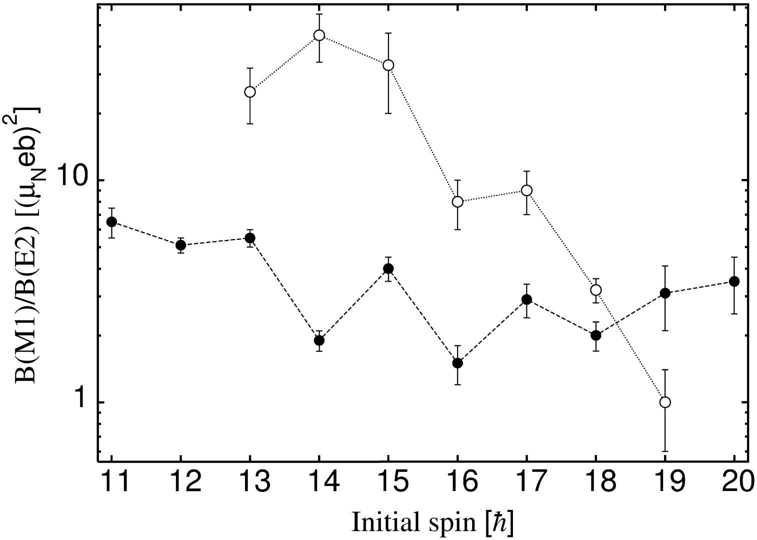

Do we have a champion?

- For cases with the smallest energy separation between doublet states, ^{134}Pr and ^{104}Rh both with $\Delta E < 50$ keV, inconsistent behaviour of the electromagnetic properties is a problem.
- In other cases, if the transition rates are all right, the degeneracy of levels is not that great.
- There is no single case which would show in a satisfactory way all properties expected of nuclear chirality.
- Various scenarios are used to explain this fact, most notably, chiral vibrations.

Band structure: ^{134}Pr

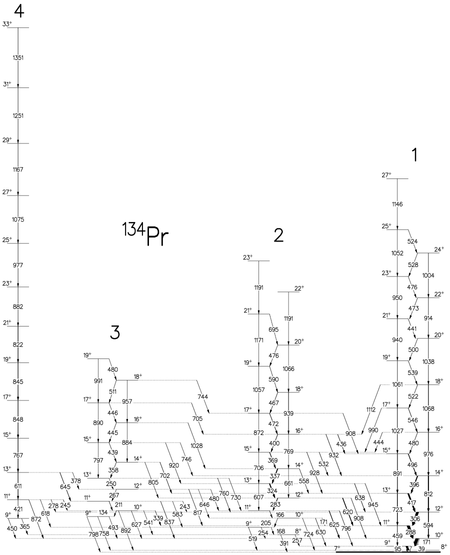

Band structure: ^{134}Pr

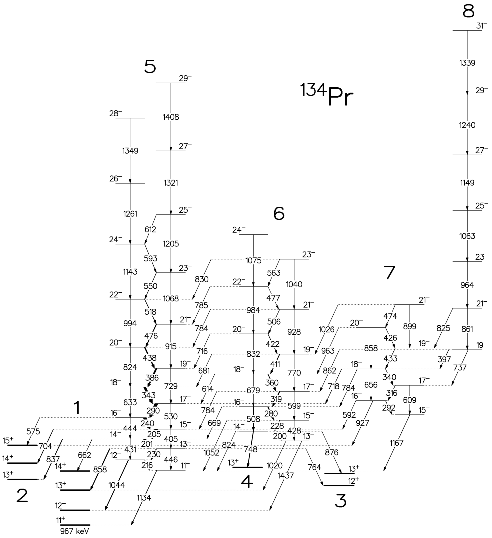

Band structure: ^{134}Pr

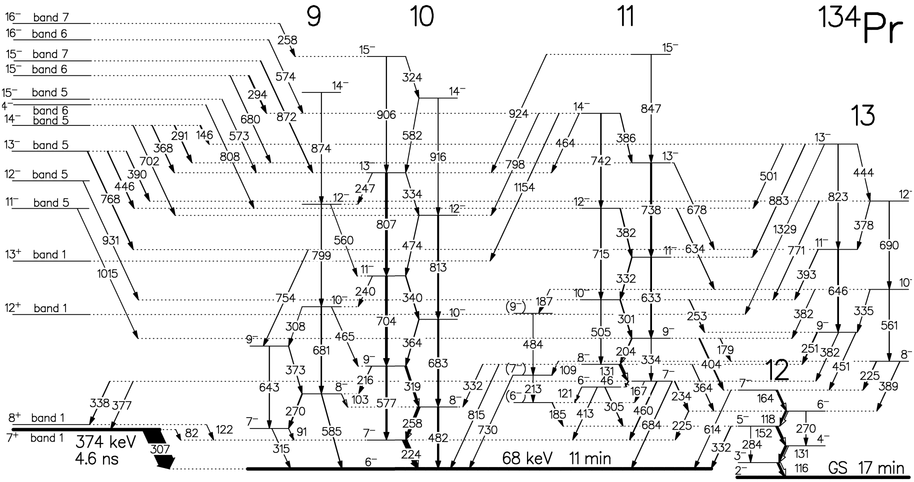

Spin and parities

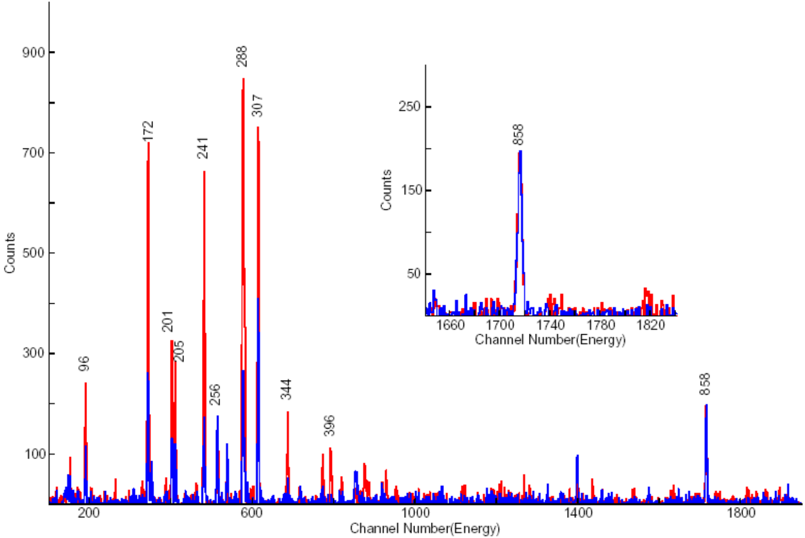

Bandhead magnetic moments

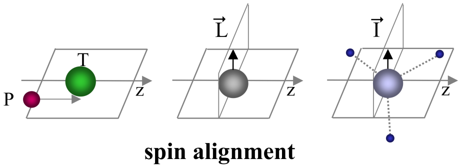

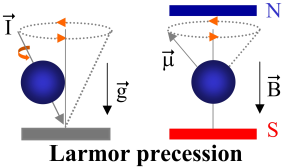

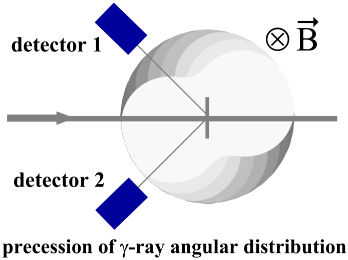

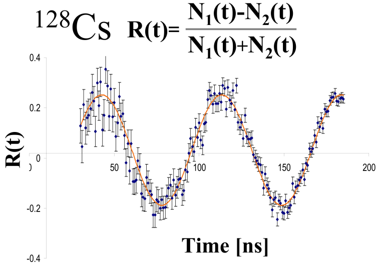

Can we nail it down?

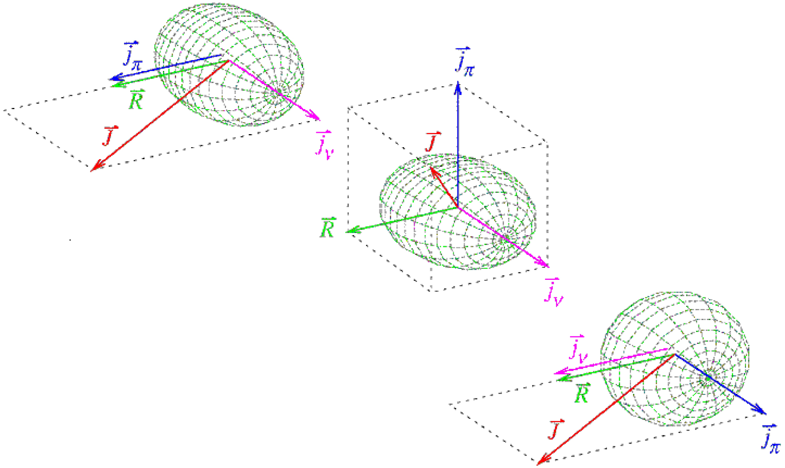

Can we nail it down?

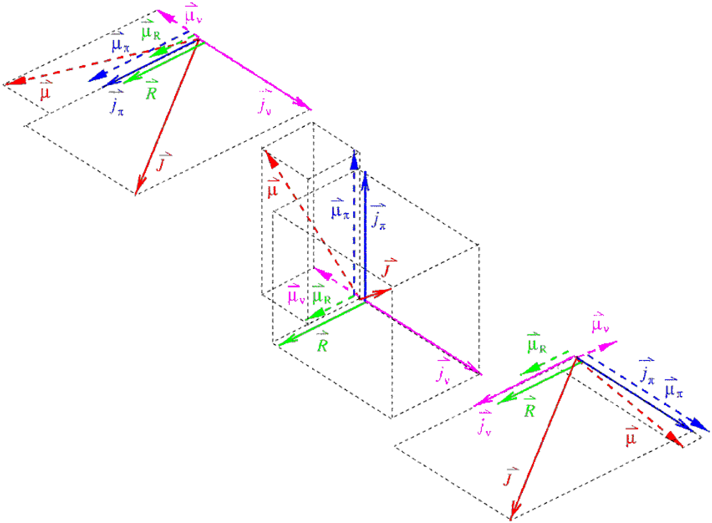

Can we nail it down?

$$g = g_R + 1/I^2[(g_{l\pi} - g_R)\vec{I}\cdot\vec{j}_\pi + (g_{l\nu} - g_R)\vec{I}\cdot\vec{j}_\nu + (g_{s\pi} - g_{l\pi})\vec{I}\cdot\vec{s}_\pi + (g_{s\nu} - g_{l\nu})\vec{I}\cdot\vec{s}_\pi]$$

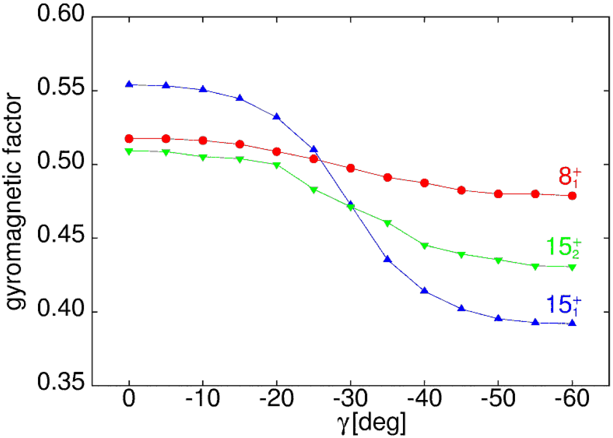

Can we nail it down?

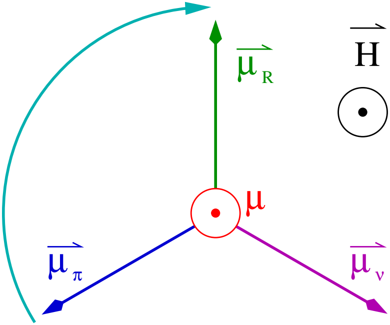

TRIUMF 500 MeV proton cyclotron

TRIUMF 500 MeV proton cyclotron

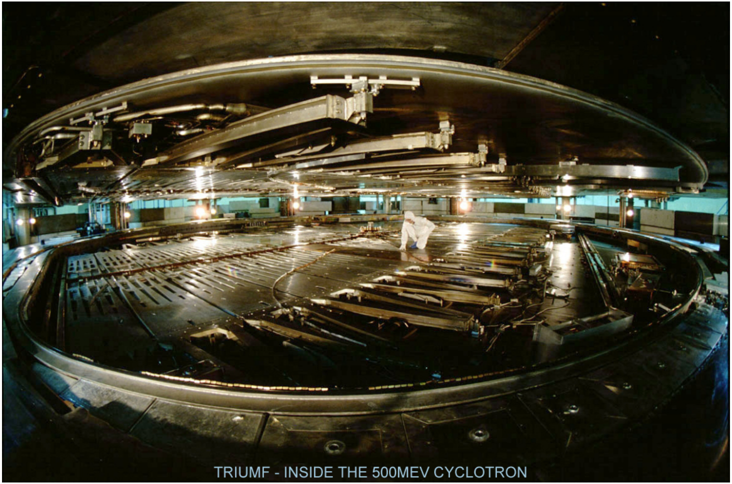

Isotope Separator and ACcelerator (ISAC)

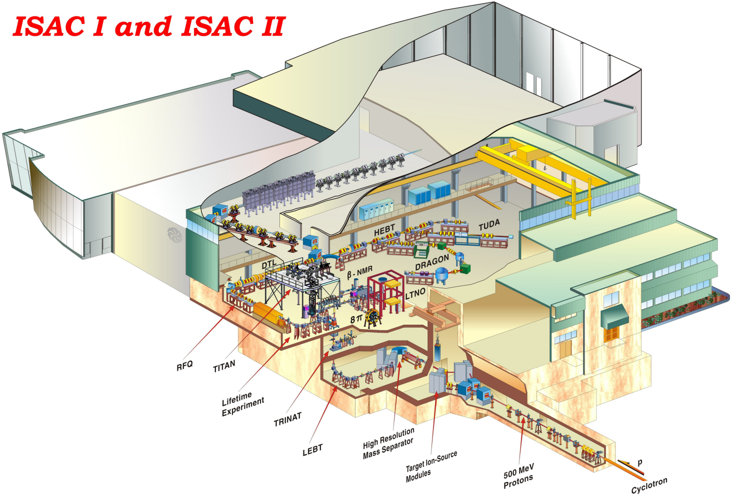

TRIUMF-ISAC Gamma-Ray Escape Suppressed Spectrometer (TIGRESS)

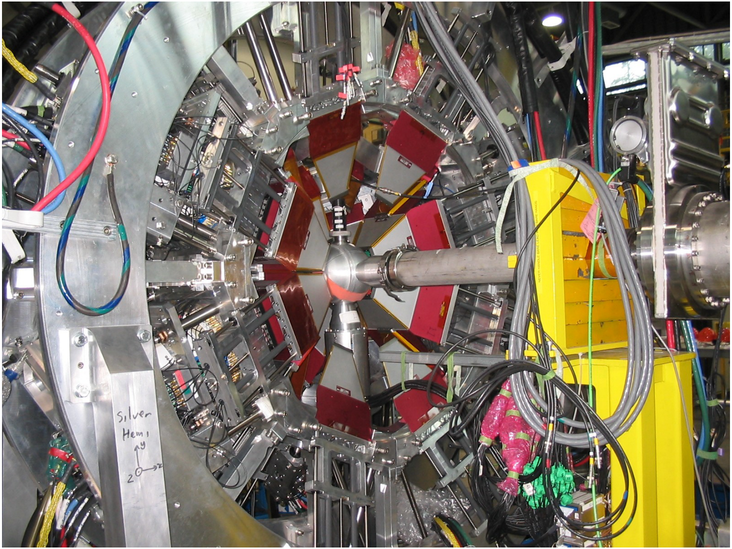

TIGRESS Integrated Plunger (TIP) project

- Designed for implementation of Doppler-shift lifetime measurements at TIGRESS.
- Combines a plunger apparatus for positioning of a target and a stopper with detection of reaction product.
- Can accommodate backed and thin targets instead of the plunger.
- Allows experiments using various nuclear reaction mechanisms to be run in a single setup.
- Has been designed by R. Henderson and the Detector Engineering Group at TRIUMF
- Has been fabricated by the SFU Science Mechanical Shop, with assistance of the TRIUMF scintillator shop.

Relativistic Doppler effect

- Motion of a source changes wavelength of emitted light.

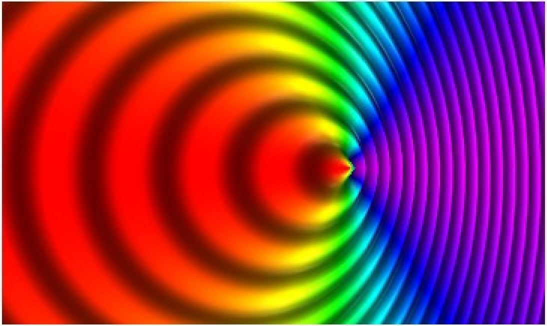

- Change in wavelength implies change of frequency and energy

$$E = E_0 \frac{\sqrt{1-\beta^2}}{1-\vec{e}\cdot\vec{\beta}} \qquad \beta = \frac{v}{c}$$

Recoil Distance Method (RDM)

c=300 μm/ps $\beta \sim 0.03$ 1 ps∼10 μm 10 ps∼100 μm

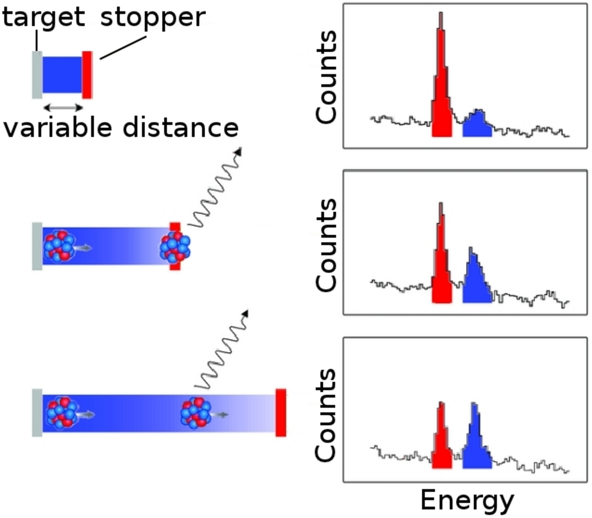

Doppler Shift Attenuation Method (DSAM)

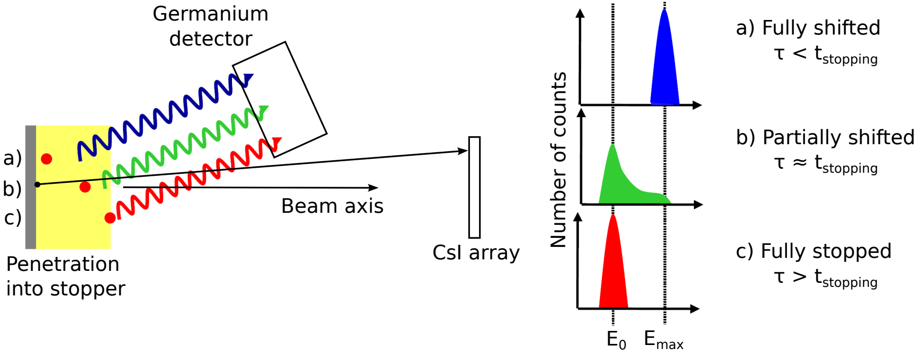

Structure information from E/M transition rates

- Electromagnetic transition rates provide experimental information for studies addressing the major scientific questions in nuclear structure.
- For γ-ray decay of excited states
  - Reduced probability $B(E2)$ for the electric quadrupole ($E2$) transition is sensitive to collective effects related to quadrupole deformation of nuclear charge distribution.
  - Reduced probability $B(E1)$ for the electric dipole ($E1$) transition is sensitive to the nuclear charge distributions.
  - Reduced probability $B(M1)$ for the magnetic dipole ($M1$) transition is sensitive to nuclear current distributions.

Advantages

Doppler-shift methods for lifetime measurement have many advantages:

- Rely on relative measurements - the decay kinetics is measured directly.
- Impact parameter does not matter —
  — decays are measured instead of excitations!
- Have relatively simple dependence on reaction kinematics.
- Are not limited by contamination of the beam.
- RDM can be applied to lifetime measurements in 1 – 500 ps range.
- Extension to sub-picoseconds range is opened through the DSAM.

TIGRESS Integrated Plunger (TIP)

Consists of:

- a vacuum vessel,
- a plunger apparatus,
- two-position target wheel with tuning apertures,
- CD-type Double Sided Silicon strip Detector (DSSD),
- forward-wall PIN diode array,
- forward wall CsI array,
- CsI ball, designed with some parts fabricated.

TIP and TIGRESS

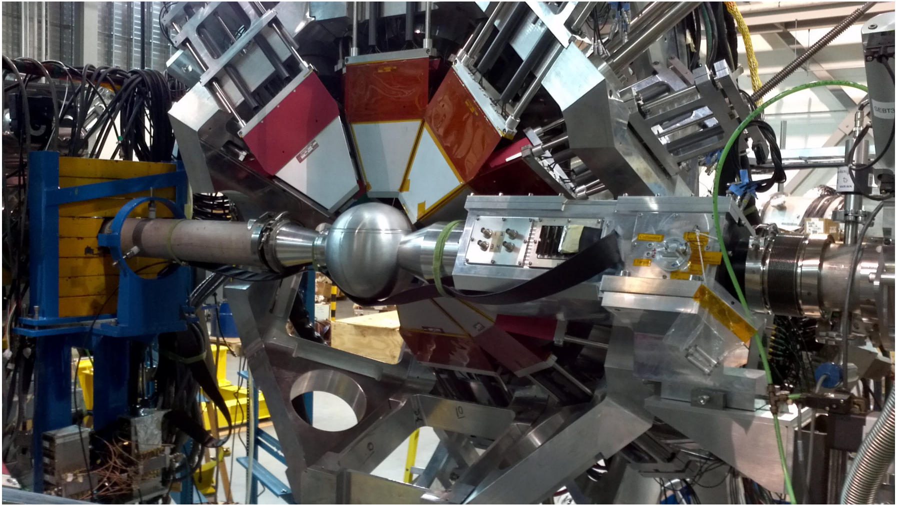

P. Voss *et. al.*, NIM A746 (2014) 87.

TIP plunger

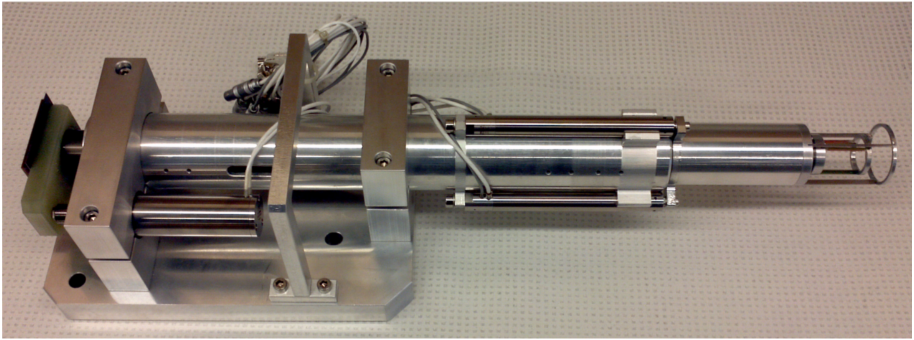

P. Voss *et. al.*, NIM A746 (2014) 87.

TIP DSAM target wheel

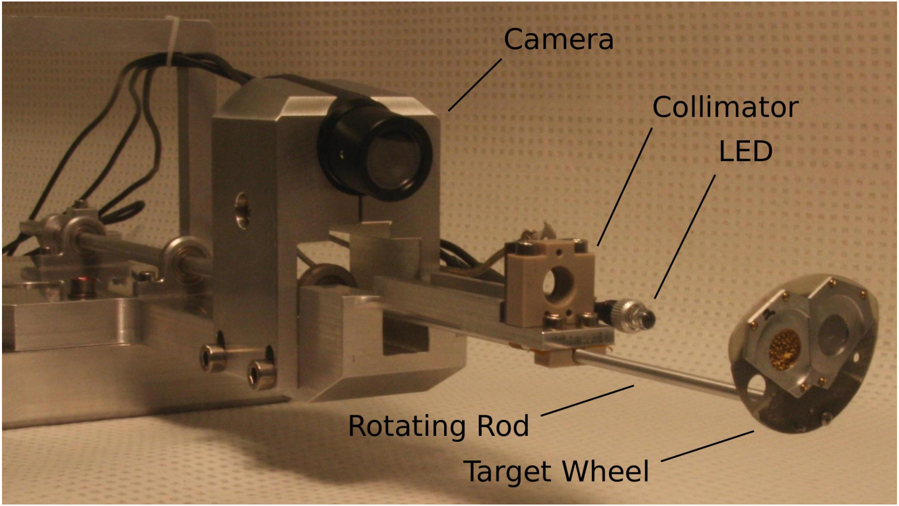

P. Voss *et. al.*, NIM A746 (2014) 87.

TIP detector mount

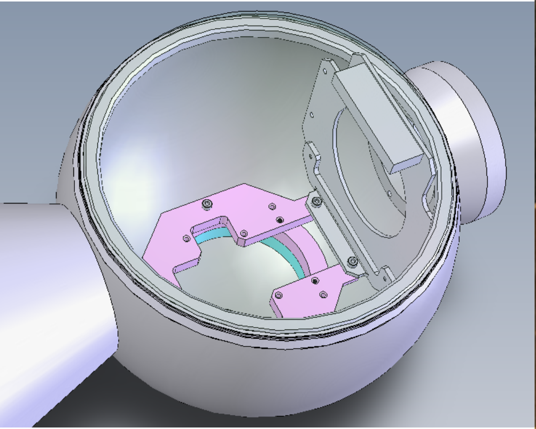

TIP charged-particle detectors

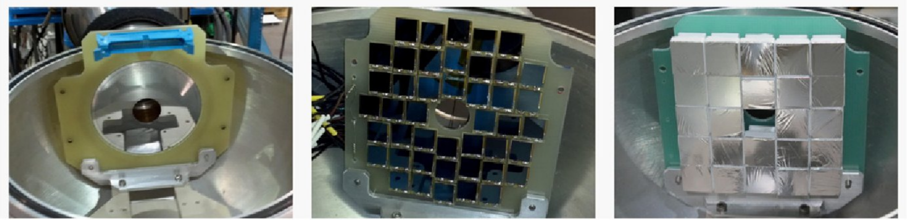

P. Voss *et. al.*, NIM A746 (2014) 87.

TIP charged-particle detector spectra

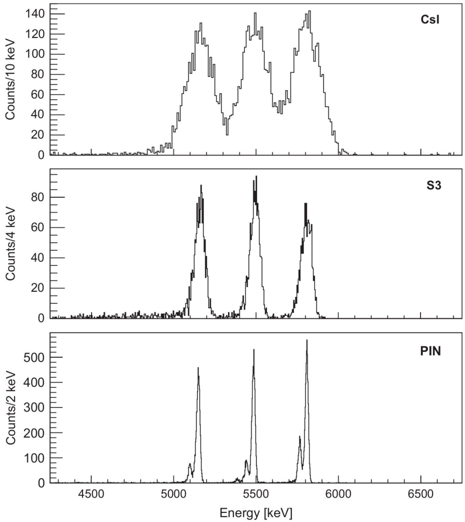

P. Voss *et. al.*, NIM A746 (2014) 87.

CsI ball design

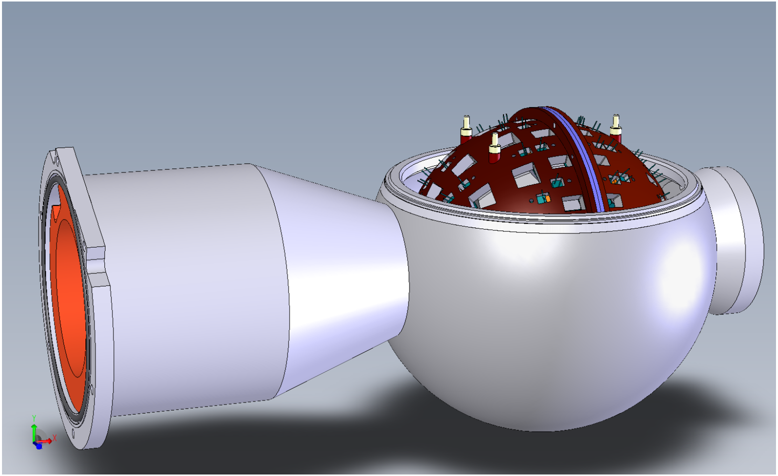

CsI ball design

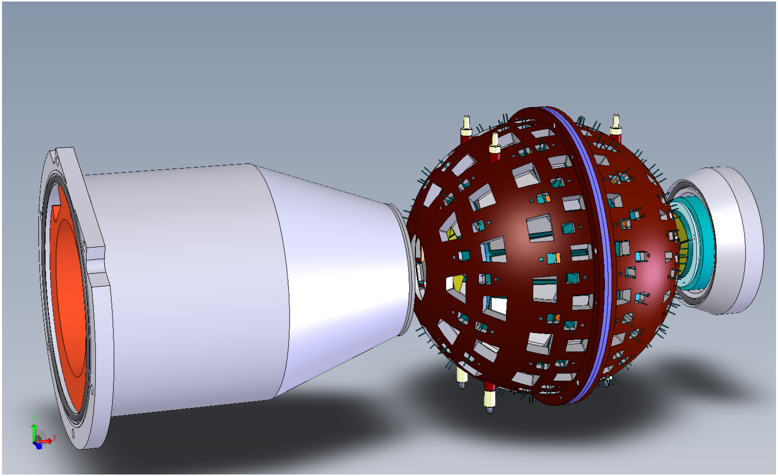

CsI ball design

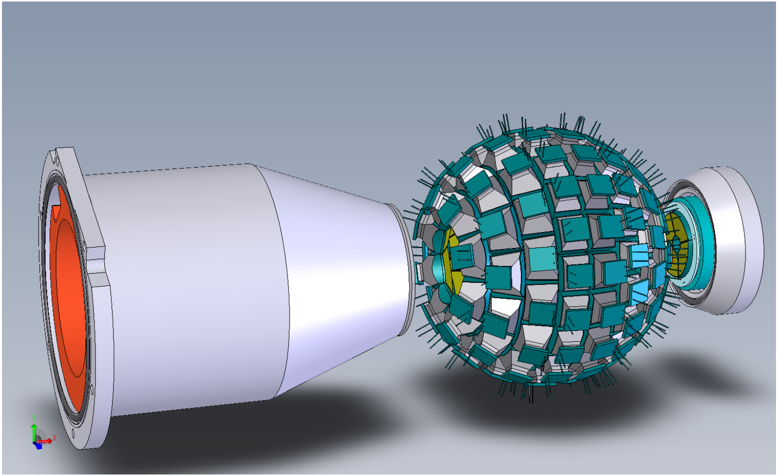

CsI ball design

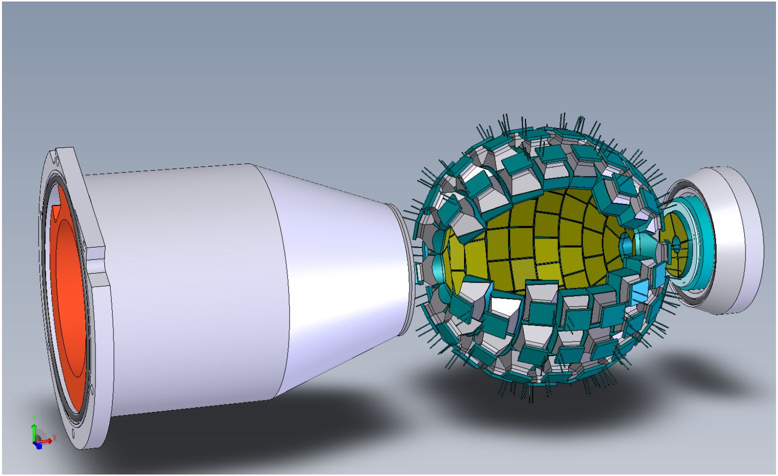

CsI ball design

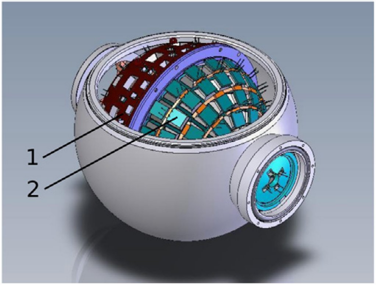

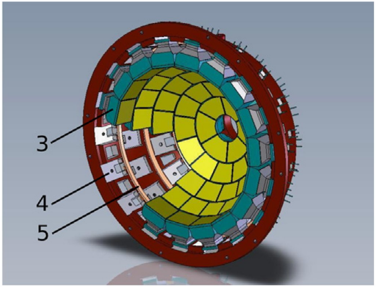

CsI ball 3D printed support structure elements

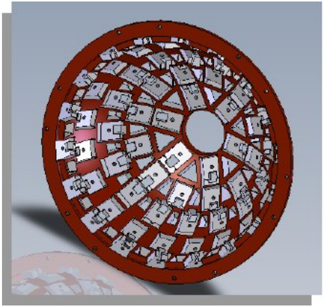

^{36}Ar DSAM using PIN diode wall.

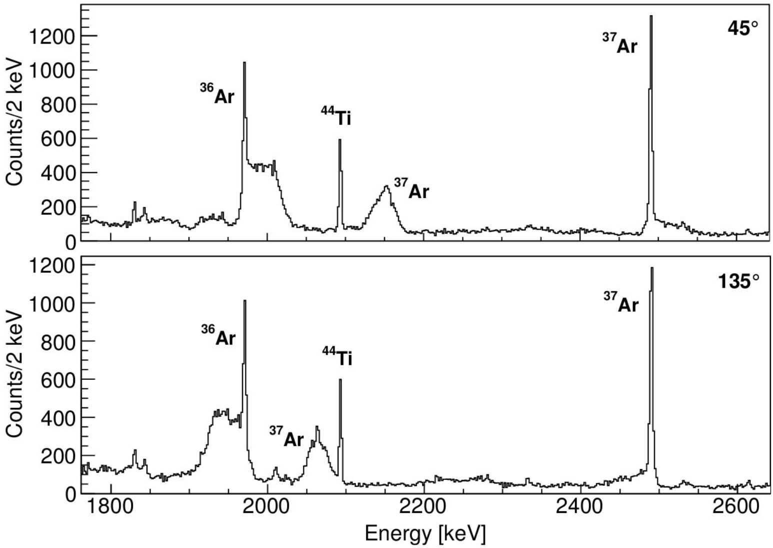

^{36}Ar DSAM PIN pulse shape sensitivity.

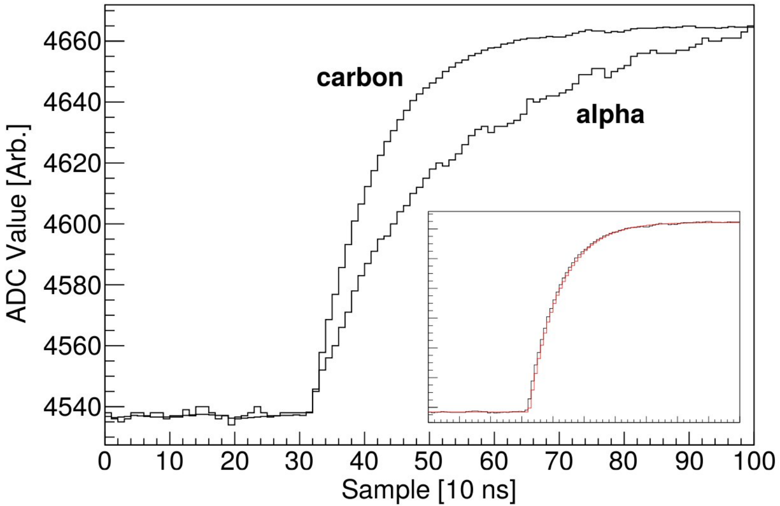

^{36}Ar DSAM PIN pulse shape sensitivity.

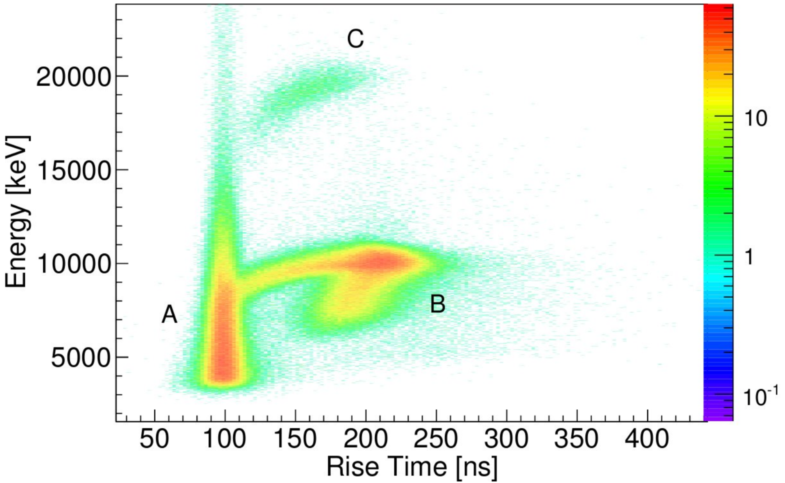

^{36}Ar DSAM PIN pulse shape sensitivity.

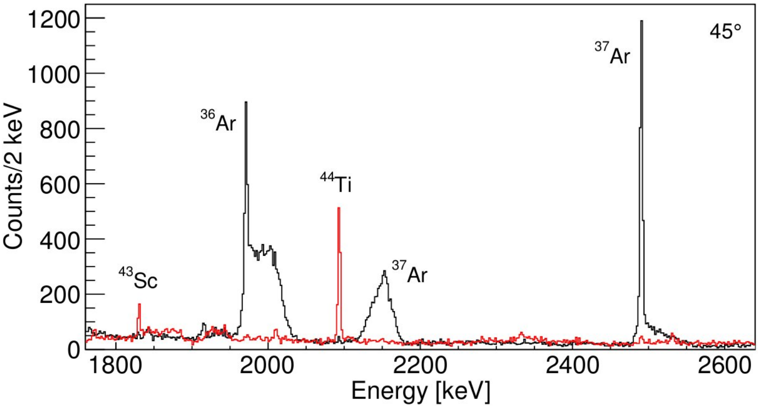

^{36}Ar DSAM PIN pulse shape sensitivity.

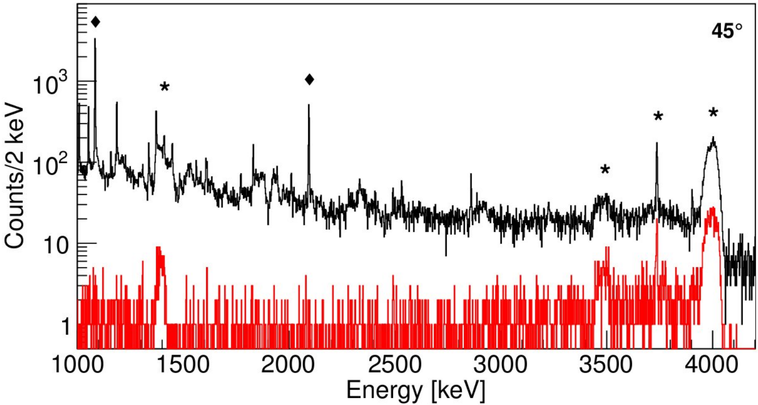

S1467: RDM TIP/TIGRESS experiment

- TIP run with the plunger and the 24-element CsI wall positioned 51.7 mm downstream from the plunger stopper.
- TIGRESS run with 16 detectors in the high-efficiency configuration.
- ^{94}Sr beam is delivered at 360 MeV (3.83 MeV/u) to a 2.0 mg/cm^2 polyethylene plunger target and 7 mg/cm^2 gold plunger stopper.
- The Coulomb barrier for ^{94}Sr on ^{12}C is 353 MeV in the LAB.
- The Coulomb barrier for ^{96}Sr on ^{197}Au is 513 MeV in the LAB.
- Beam projectiles are excited through the partially unsafe Coulex process on carbon in the polyethylene target.
- The unreacted beam passes through the plunger target and stopper to the screened TIGRESS beam dump.

S1467: RDM TIP/TIGRESS experiment

- Recoiling carbons from the Coulex process are detected in the TIP CsI wall providing the reaction tag for the trigger and are identified off-line through the Pulse Shape Analysis.
- Excited projectile from the Coulex are stopped in the stopper.
- The Coulexed projectile speed is sufficient to distinguish between the doppler-shifted gamma-ray decay in flight from the decay at rest.
- Coulexed projectile gamma-ray decays are detected by TIGRESS at 6 different angles with respect to the axis to the incoming beam.
- The trigger for the DAQ is provided by a logic AND of a single CsI and a single TIGRESS detector identifying Coulomb excitations on carbon as gold recoils are not energetic enough to trigger a CsI detector.

S1467: Issues to address

- Reaction yields.
- Gamma-ray energy separation between the in-flight and at-rest decays.
- Suppression of CsI wall hits by the unreacted beam while maintaining detection efficiency for the target recoils.
- Accumulation of radioactivity in the TIGRESS field of view, including the CsI wall.

GEANT4 TIP/TIGRESS for analysis and planning

- The structure of the code and the method of implementing user-defined reaction mechanism followed by gamma-ray decay based on Adrich *et al.* NIM A598 (2009) 454.
- The Coulex kinematics, cross sections, angular distributions and correlations implemented based on analytic solutions for the single-step $E2$ process as defined in Alder *et al.* Rev. Mod. Phys. 28 (1956) 432.
- Various TIP sensitive charge-particle detectors implemented.
- Gamma-ray sensitive detectors ported from the GRIFFIN/TIGRESS code originating from Guelph.
- Data analysis implemented using ROOT
- GEANT/ROOT interface used for interactive or batch operations.

TIP plunger and CsI wall

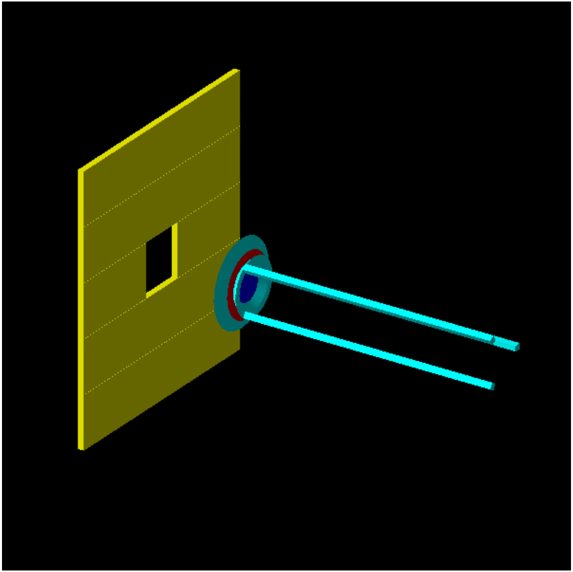

TIP plunger, CsI wall, single TIGRESS CSS

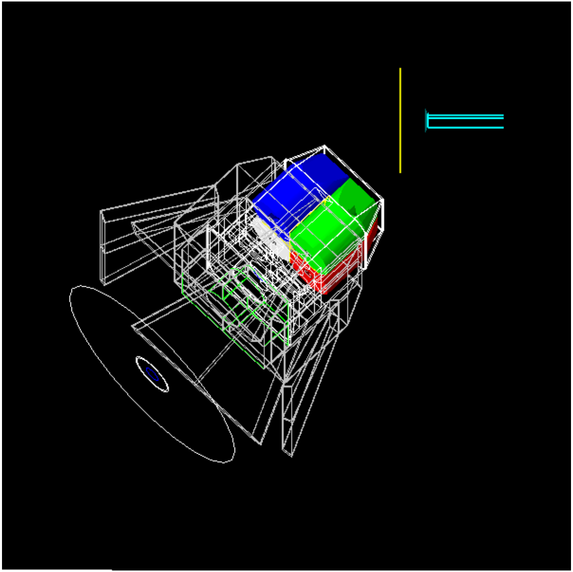

TIP plunger, CsI wall, and TIGRESS

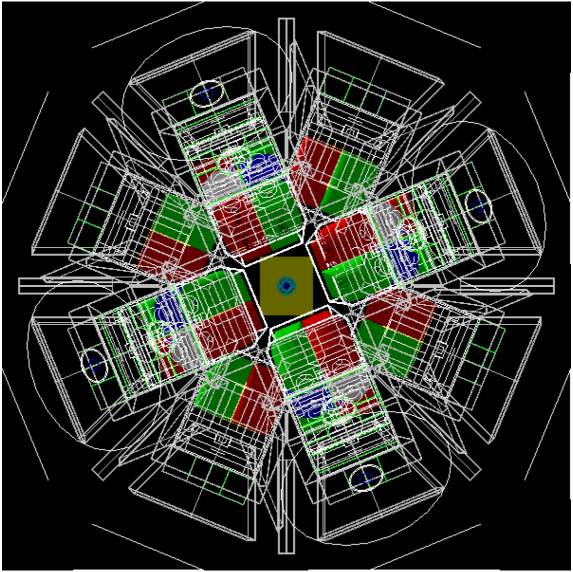

Thick target Coulex in the GEANT4 framework

- Coulomb cross sections depend on the Centre of Mass energy and through the impact parameter on the scattering angle.
- For realistic calculations the impact on the reaction yield of the beam energy loss while traversing the target needs to be accounted for.
- While analytic solutions exist for a single-step Coulex at a given Centre of Mass energy an efficient integration over a thick target is needed for the calculations to be useful.
- This issue can be resolve well through track weighting mechanism provided by GEANT.

Coulex cross section vs. target depth

RED/BLUE is with/without the energy loss correction to the cross section

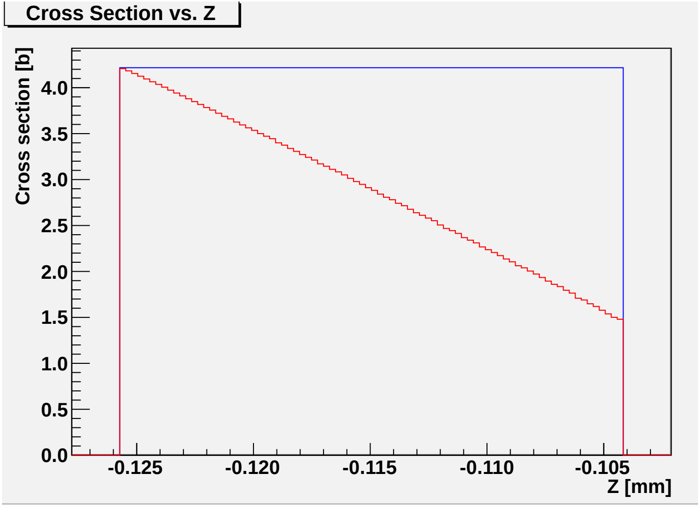

Angular coverage of the CsI/TIGRESS setup

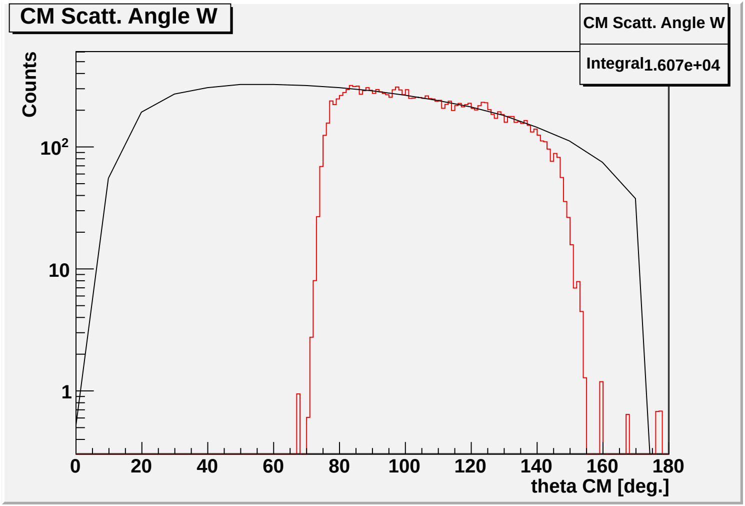

Target-stopper separation of 200 μm, 45°

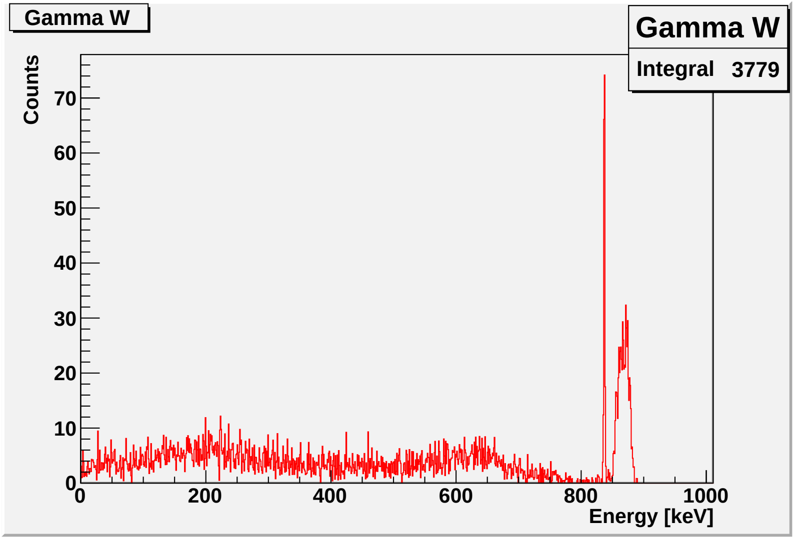

Target-stopper separation of 200 μm, 90°

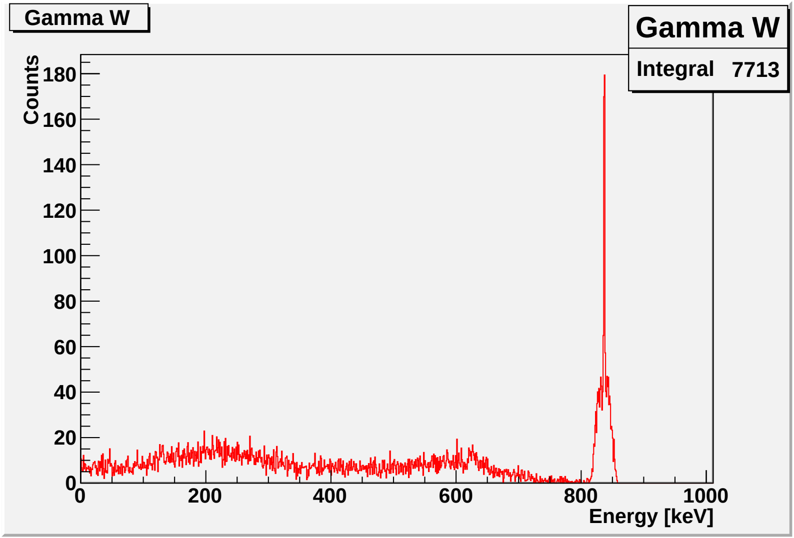

Target-stopper separation of 200 μm, 135°

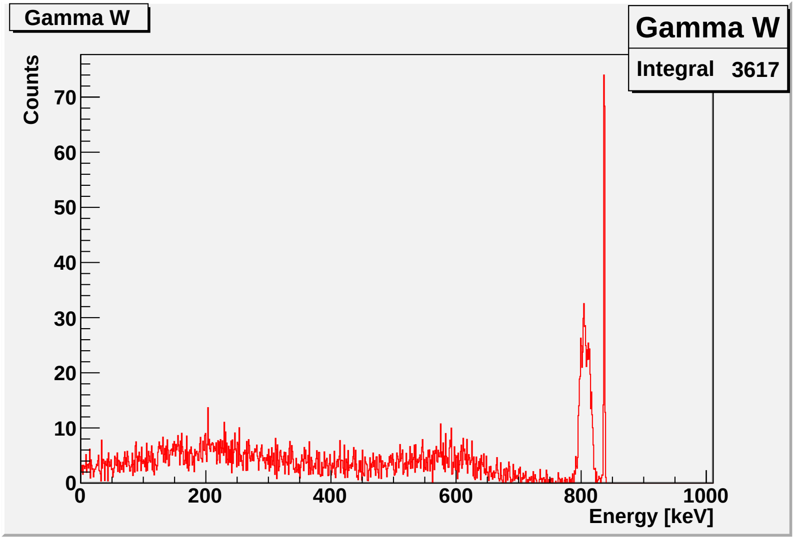

Speed of ^{94}Sr at the de-excitation

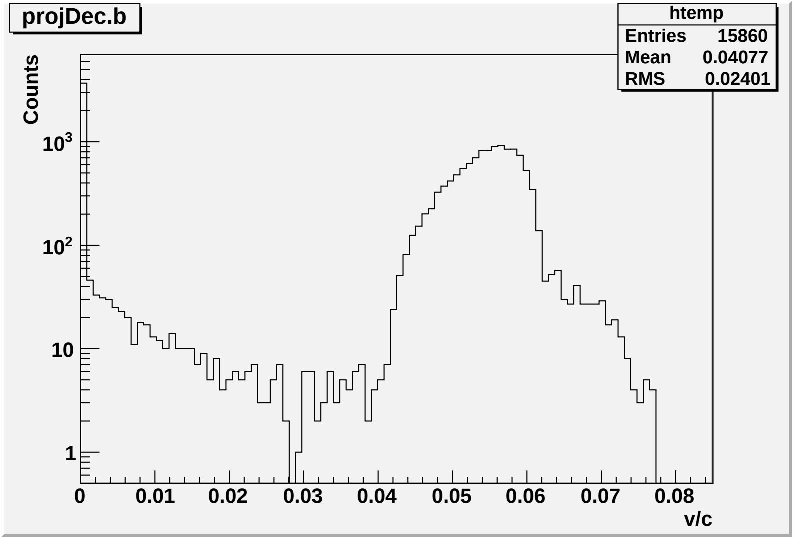

^{12}C recoil energy in CsI ring 1

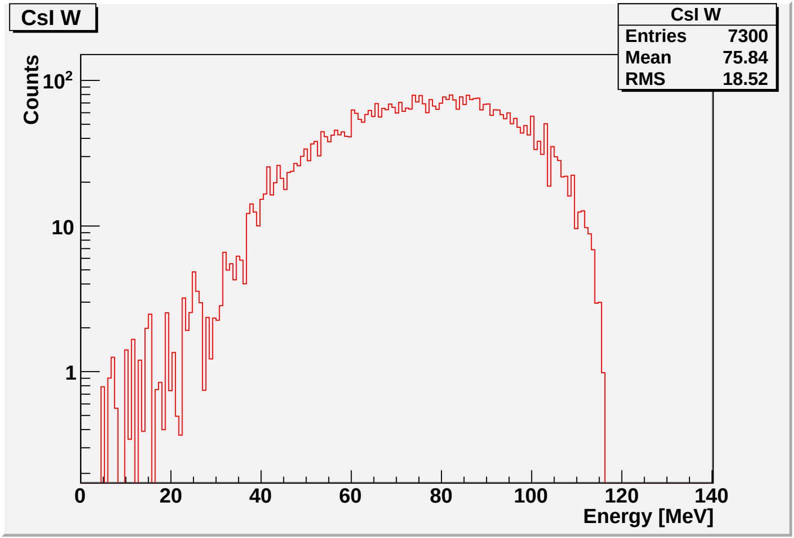

^{12}C recoil energy in CsI ring 2

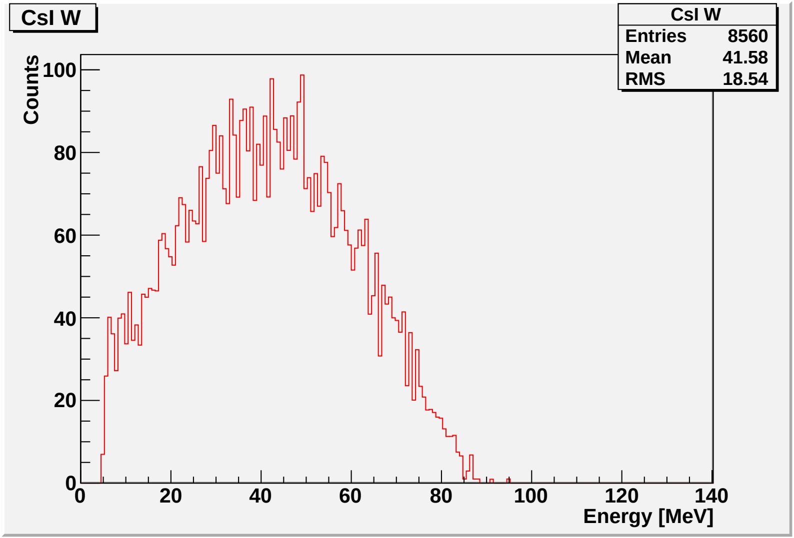

Unreacted beam energies downstream from the stopper

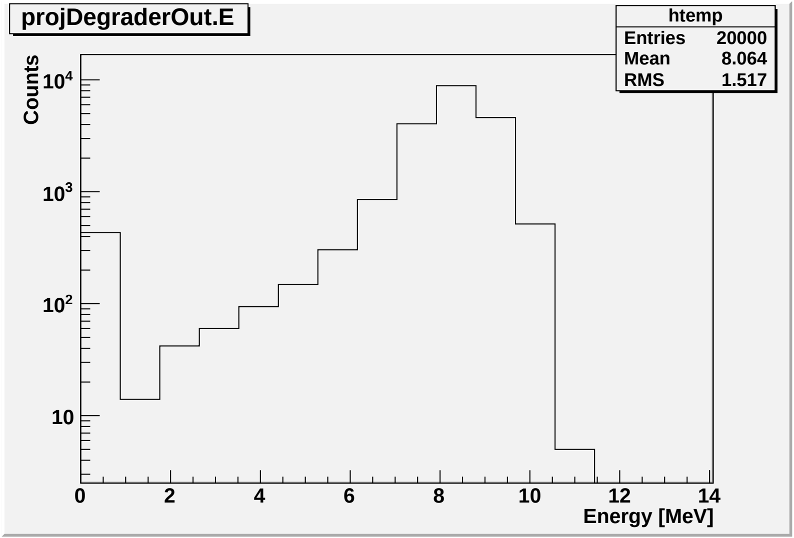

Unreacted beam hits in the CsI wall

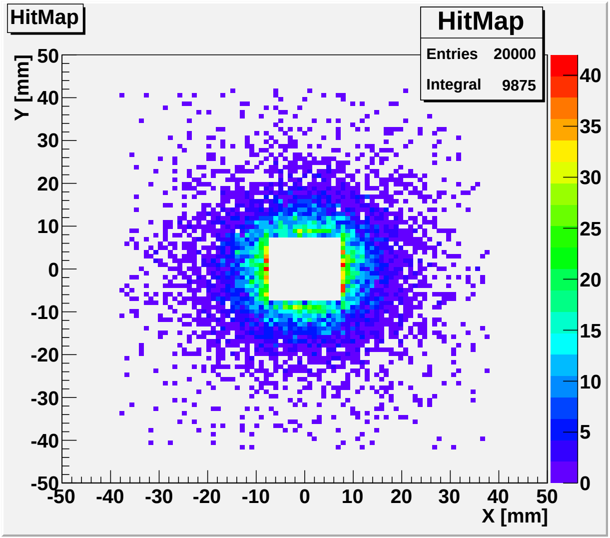

Possible experiments

Isomeric bandheads:

- masses in the TITAN Penning trap
- β-decay lifetimes/spins in the GRIFFIN or 8π
- magnetic moments through β-induced NMR
- quadrupole moments through β-induced NQR
- transfer/pick-up reactions

High-spin states:

- Coulomb excitations
- lifetimes
- angular correlations
- perturbed angular correlations through recoil into vacuum

Can we find the smoking gun?